R. & M. No. 3436

MINISTRY OF AVIATION

AERONAUTICAL RESEARCH COUNCIL
REPORTS AND MEMORANDA

An Analysis of the Subsonic Flow past Symmetrical Blunt-Trailing-Edge Aerofoil Sections at Zero Incidence, in the Absence of a Vortex Street

By J. F. Nash

LONDON: HER MAJESTY'S STATIONERY OFFICE
1966

PRICE 16*s*. 0*d*. NET

An Analysis of the Subsonic Flow past Symmetrical Blunt-Trailing-Edge Aerofoil Sections at Zero Incidence, in the Absence of a Vortex Street

By J. F. NASH

*Reports and Memoranda No. 3436**
August, 1964

Summary

A simplified analysis is presented of the subsonic non-periodic flow past symmetrical blunt-trailing-edge sections at zero incidence. The pressure distribution is determined, with the base pressure as parameter, by an analysis of the inviscid flow past a displacement surface representing the section, the attached boundary layer, and the wake. The shape of the downstream part of the displacement surface presented by the wake is specified by pressure criteria established from a study of the pressure distribution downstream of a rearward-facing step.

The solution is rendered unique by the estimation of the base pressure. An analysis is made of the flow in the wake, invoking the condition that the wake momentum thickness must asymptote to a value at infinity downstream which is proportional to the total drag of the section. The viscous solution can be regarded as a logical extension to blunt-trailing-edge sections of the method of Squire and Young for the estimation of the drag of conventional aerofoils.

A few examples are submitted to illustrate the application of the method.

LIST OF CONTENTS

* Replaces N.P.L. Aero Report No. 1112—A.R.C. 26 117. Published with the permission of the Director, National Physical Laboratory.

1. *Introduction.*

1.1. *The Nature of the Problem.*

The problem of predicting the pressure distribution round conventional aerofoil sections at subsonic speeds has to a large extent been solved. For sections of small thickness-chord ratio at moderate angles of incidence, attached flow can generally be preserved to a point at, or near, the trailing edge, and in many applications consideration of the potential flow past the section (with, perhaps, some correction to the theoretical lift-curve slope) yields a pressure distribution which is sufficiently close to that of the real flow to make any higher approximation unnecessary. Nevertheless, the real flow is distorted from the inviscid pattern by the displacement effect of the boundary layer and if accurate predictions of the pressures are required, particularly near the trailing edge, the analysis must be taken a stage further. Methods are now available for the solution of the viscous flow past two-dimensional aerofoils (*see*, e.g. Thwaites[1]), usually based on parallel calculations of the development of the boundary layer and of the potential flow past the displacement surface. Iterative procedures are generally employed but under normal circumstances the methods converge rapidly and only one or two iterations are apparently required. However the validity, and satisfactory convergence, of such methods necessarily depend on the absence of significant regions of separated flow on the section.

In cases where separation is a significant feature of the flow pattern, methods of this type are difficult to apply for a number of reasons.

Firstly, when attached flow is no longer achieved the uniqueness of the flow pattern deteriorates. The existence of regions of separated flow presents a degree of freedom which often results in unsteady phenomena. Typical examples of this are the buffeting experienced on aerofoil sections with rear separation, and, in the present context, the formation of a vortex street in the wake of a blunt-trailing-edge aerofoil section. Thus in any particular case it is first necessary to establish the relevance and validity of a steady-flow analysis. This point will be discussed later in relation to blunt-trailing-edge sections (Section 1.2 below).

Secondly, if, in spite of the existence of regions of separation, the flow can be considered to be non-time-dependent the complexity of the problem lies in the fact that the shape of part of the displacement surface is initially unknown. Nor, in this case, can it be assumed even as a first approximation for iteration purposes that the displacement surface coincides with the section. The literature (*see*, e.g. Woods[2]) contains numerous examples of the analysis of flows with separation using 'free-streamline' models. In these methods, on the parts of the displacement surface representing the separated regions (the 'free streamlines' as they are usually termed), information is given regarding the pressures. The problem is thus specified by mixed boundary conditions, and the 'solution' is represented by the computed potential flow outside the displacement surface. The analysis of flow models of this type started many years ago with the work of Kirchoff, Helmholtz, Joukowski and others, and is still being actively pursued. The analytical methods have reached an advanced state of sophistication and it is now possible to treat problems of general section geometry and to impose arbitrary pressure distributions along the free streamlines[2]. The application of this work has been largely to cavitating hydrofoils[3, 4]. In this instance the condition of constant pressure along the free streamlines is realistic, and the value of the pressure in the cavity is known at the outset in terms of the vapour pressure of the liquid. In aerodynamic applications, however, the pressure in the separated region must be determined as part of the solution, and pressure variations through the region are frequently too significant to be ignored[5, 6]. Thus the formal solution of the

external inviscid flow does not represent an explicit solution of the problem as a whole, and the pressure conditions on the 'free streamlines' remain to be determined by some other means.

In the case of an aerofoil section with separation it would appear that the indeterminacy can be removed only by a consideration of the viscous/turbulent processes in the separated region. In its most general formulation the complete solution would involve the simultaneous analysis of (a) the external inviscid flow and (b) the viscous flow, with compatibility conditions satisfied at all points on the displacement surface. As in the analysis of the viscous attached flow over an aerofoil, the pressure distribution considered in the inviscid solution must be such as to be consistent with the growth of the boundary layer (attached and separated) to produce the appropriate displacement surface. Paying heed to the problem of predicting the development of separated boundary layers in an arbitrary pressure distribution, it can be appreciated that the analytic and computational difficulties would indeed be formidable.

Nevertheless, there is scope for the development of approximate methods with a limited range of validity, and it is in this context that the present work is considered to make a contribution. It would seem that in two particular respects restrictions must be placed on the generality of the problem. Firstly, the range of possible solutions of the external inviscid flow must be narrowed down. This could be attempted by expressing typical pressure distributions through the separated region on some sort of similarity basis in terms of a convenient number of disposable parameters. The particular inviscid solution corresponding most closely to physical reality would then be selected according to the extent to which it was compatible with the development of the viscous region. Secondly, the demands of the compatibility criteria must be limited in such a way as to be accommodated by a tractable viscous analysis.

1.2. *Blunt-Trailing-Edge Aerofoil Sections.*

The choice of an aerofoil section of non-zero trailing-edge thickness can be made for one of several reasons, either structural or aerodynamic. In the latter context the choice may be made on the basis of the aerofoil performance at supersonic speeds[7]. (For a swept wing this will refer to the Mach number component exceeding unity normal to some typical sweep angle.) In this case the need for information on the subsonic characteristics arises in connection with the off-design performance. Alternatively, the use of a blunt trailing edge has been suggested[8] as a possible means of delaying the onset of shock-associated phenomena (drag-rise, shock-induced separation, etc.) at high subsonic speeds. In this case the subsonic phase is clearly of prime importance. In both these instances advantages are envisaged from the improvement in the design of the section which can be realised by relaxing the condition of zero trailing-edge thickness. The advantages are nevertheless obtained at the expense of not preserving attached flow over the rear of the section. At subsonic speeds the acceptance of this separation incurs the loss of pressure recovery, and the base pressure which acts on the blunt trailing edge is frequently low making a significant contribution to the drag of the aerofoil.

In general the flow past a two-dimensional blunt-trailing-edge aerofoil section at subsonic speeds is dominated by periodic effects and the formation of a vortex street[9]. The concentrations of vorticity in the wake represent a sizeable energy loss which is transmitted to the section partly as a depression of the base pressure relative to that which could be supported by a non-periodic wake, and partly as a further decrease of the pressures on the part of the aerofoil surface within the region of influence of conditions at the trailing edge. The vortex street is thus a major factor in the development of the

drag, and its suppression is one of the principal objectives if the potential advantages of sections of this type are to be usefully exploited. The use of a splitter-plate[6, 10, 11, 13] or trailing-edge cavity[6, 12], a high-velocity jet at the trailing edge[11], base bleed[14, 15, 16], or suction[12, 17], all serve to reduce the strength of the vortex street with various degrees of success, and further work is in progress on some of these devices.

In this context the steady condition represents the optimum at which efforts to inhibit the periodicity are directed. An analysis of the non-periodic base flow is thus relevant in this connection but also has a bearing on other problems and may provide useful information on the characteristics of flows which do not exhibit periodic phenomena as a significant feature. Among such problems are the flow past two-dimensional aerofoils (and three-dimensional wings) with closed separation bubbles, the flow past three-dimensional bodies with base area, and also various interaction problems involving the mixing of jets or of a jet with an external stream. Even the simple case of the flow past a step has an important relevance to a number of problems both in aeronautics and in other branches of engineering.

1.3. *The Object and Limitations of the Present Work.*

The object of the present work is thus to analyse the (strictly-speaking hypothetical) flow past a particular type of aerofoil section with separation—i.e. the section with a non-zero trailing-edge thickness. The flow is assumed to be attached over the whole of the aerofoil surface up to the trailing edge but then to separate leaving the rearward-facing area in a separated-flow region. The study is restricted to the case of the symmetrical section at zero incidence, and to the case of a turbulent wake.

It will be the intention of future work to extend the analysis to lifting aerofoils but there are still important gaps in our understanding of this problem—particularly regarding the factors which control the circulation.

Essentially, the method is divided into two parts: an analysis of the quasi-inviscid external flow, and an analysis of the turbulent flow in the wake. Between them the two analyses yield a unique solution for the base pressure, the complete pressure distribution over the section and the profile drag.

The problem of the external flow is of the 'free streamline' type. An important difference exists, however, between the present problem and that of the classical 'bluff section'; this is concerned with the displacement effect of the attached boundary layer. In contrast to the 'bluff section' problem, the displacement thickness of the boundary layer cannot, in general, be neglected in comparison with typical section dimensions. This presents a difficulty since the geometry of the upstream part of the displacement surface (i.e. that corresponding to the aerofoil and the attached boundary layer) is not known precisely at the outset but must be determined as part of the solution. In this respect the problem is similar to that of calculating the viscous flow past a conventional aerofoil section (*see* Section 1.1 above), and the difficulty is overcome in the same way—by an iterative procedure. In the present case, however, the iteration converges, not to the final solution, but to one possible solution of the external flow corresponding to a particular value of the base pressure. The solution of the problem as a whole remains indeterminate until the solution of the external flow is matched to that of the wake.

These remarks apply to the direct problem of predicting the characteristics of a given aerofoil. In the indirect, or design, problem the difficulty regarding the boundary-layer growth would not

arise. The pressure distribution over the section (or, more precisely over the upstream displacement surface) would be given and the external flow would be completely specified in terms of the base pressure by imposing on the wake a pressure distribution of the type considered in the present work. The geometry of the upstream displacement surface could then be determined. With the surface pressure distribution known the boundary-layer development could be computed and the section geometry derived without any need for an iteration. Thus the indirect problem can be regarded as solved in principle, but it will not be considered further in this paper.

1.4. *Relevance of Methods Appropriate to Supersonic Flow.*

For the supersonic case, successful methods for the prediction of base pressures have been developed[18, 19, 20] from those originally proposed by Chapman *et al*[21], Korst[22] and Kirk[23]. In these methods the pressure rise recovered in the wake ahead of the point of confluence has been related to the velocity imparted to fluid particles on the dividing streamlines by mixing in the free-shear layers. The pressure recovery accommodated by the wake downstream of the point of confluence has been assessed either empirically[18, 20] or by a semi-empirical analysis of the rehabilitation of the wake velocity profile[19]. Since the wake pressure must eventually recover to free-stream static pressure far downstream, the determination of the total pressure rise represents a solution for the base pressure.

The validity of the method of Ref. 18 has been demonstrated in subsonic flow but the difficulties associated with the estimation of the downstream wake pressure recovery, either empirically or analytically, would seem to preclude the development of the method for general application.

2. *The Flow Model.*

2.1. *The Wake.*

The flow model considered in the present analysis is illustrated in Fig. 2. The flow is assumed to separate at sharp corners at the trailing edge but to have remained attached over the whole of the aerofoil surface ahead of the trailing edge. The most elementary streamline pattern which can be constructed to satisfy the flow conditions immediately downstream of the trailing edge is shown in Fig. 3. A slowly-circulating vortical flow, or weak eddy is assumed to form on each side of the wake centre line, and the presence of this pair of standing eddies demands the existence of a free stagnation point which will be referred to as the 'point of confluence'. If mass is neither added to, nor extracted from, the region, a single streamline will join each separation point to the point of confluence. If, on the other hand, a continuous injection of fluid is maintained through the base (base-bleed) the separation streamline will be displaced from that passing through the point of confluence to allow the bleed mass flux to escape downstream. In the present paper only the case of zero bleed will be considered. The streamline passing through each separation point and the point of confluence will be termed a 'dividing streamline'.

The fluid velocities in the separated region are assumed to be small except close to the dividing streamlines. The adjustment of velocity from the low value in the separated region to the value in the external stream will thus occur over a relatively small distance, and the flow near each dividing streamline can be regarded as a free-shear layer. The two free-shear layers, which have their origin in the boundary layers at separation, converge to form the downstream wake in a region which will be referred to as the 'region of confluence'.

Consistent with the assumption of low velocities, the pressure is considered to remain essentially constant through the separated region at a value close to the base pressure, p_b. At the downstream end of the region, however, an abrupt pressure rise takes place, associated with the confluence of the two shear layers. In general the pressure does not recover monotonically to its final value, equal to p, far downstream but exhibits an overshoot in the region of confluence (Fig. 2). The pressure overshoot is linked with the presence of the stagnation point but the point of maximum pressure does not in general correlate with the point of confluence (*see* Ref. 6).

As suggested in Section 1.1 above, the intention will be to establish simple criteria for describing the pressure distribution in the initial part of the wake, as a basis for the construction of families of solutions of the external inviscid flow. This will be done from an examination of experimental results. Although the present flow model is, strictly speaking, hypothetical, an experiment could be devised to measure the pressure distribution along the wake behind a blunt-trailing-edge aerofoil section under conditions in which the effects of the vortex street were minimised. But it is questionable whether meaningful results would be obtained and it is very likely that spurious trends would be introduced either by residual periodicity or by disturbances set up by the agency used to preserve the wake stability. Reference will therefore be made to measurements of the pressure distribution through the separated region downstream of a rearward-facing step. This at once raises the question of the relevance of these data in the present context.

For our present purpose the flow past a step, considered together with its image in the plane downstream surface, can be regarded as equivalent to that in the wake of a symmetrical blunt-trailing-edge section at zero incidence if two conditions are satisfied. Firstly, the wake must be steady such that its centre line represents a streamline. This point has already been taken into account in the formulation of the problem. Secondly, it must be assumed that the shear stress acting on the surface downstream of the step has a negligible effect on the pressure field. This has not been demonstrated rigorously, but it seems to be a plausible approximation. Through the separated region itself the skin friction is clearly small, at the reattachment point it is exactly zero and far downstream of the step it again tends to zero. At short distances downstream of reattachment the viscous layer is relatively thick and there is no evidence that shear stresses set up at the boundary would be sufficiently strong to influence the pressure field. The only direct evidence there is concerning the equivalence between the flow past a step and past a blunt trailing edge is that at supersonic speeds base-pressure data obtained from tests on steps and isolated sections correlate fairly successfully at least so long as the boundary-layer thickness at separation is not large[18]. Thus, while the equivalence between the two flows must be regarded as an approximation, it does not appear to be a serious one, and until further information is available we shall feel justified in making appeal to it.

2.2. *The External Flow.*

Criteria describing the general form of the pressure distribution in the initial part of the wake will be invoked to limit the range of possible inviscid external-flow patterns to a singly-infinite set of solutions, each corresponding to a particular value of the base pressure. Thus it will be possible to compute, in terms of the base pressure, the pressure distribution over the section, the drag and various specific conditions in the wake. The purpose of the viscous analysis will then be to determine the base pressure and render the solution unique.

The inviscid solution could be derived by any of the available methods for the treatment of mixed-boundary-value problems. Methods based on conformal transformations are the most general

but for aerofoil sections of arbitrary geometry the computational difficulties were considered to be greater than could be conveniently accommodated. It was therefore decided that the present analysis should be developed on the lines of linearised theory. The displacement surface is thus generated by a source distribution disposed along the chordline and the centreline of the wake. So long as the displacement thickness of the attached boundary layer is not large, the shape of the upstream part of the displacement surface (ahead of the trailing edge) can be regarded as known, at least approximately, and the corresponding source distribution can be determined at once. When the pressure distribution over the section is subsequently determined as a function of the base pressure, a second approximation to the boundary-layer growth can be derived, and so on. The process would appear to converge rapidly in most cases and only a few iterations are likely to be involved.

The shape of the downstream part of the displacement surface is not known initially, but is specified by information regarding the pressures on it. The strength of the source distribution representing the wake is determinable by the solution of a singular integral equation. Alternatively, a method is indicated by which the integral equation can be replaced by a set of simultaneous linear equations.

3. *Outline of the Method.*

The present method makes use of the fundamental result that, in two-dimensional subsonic flow, the wake momentum thickness tends to a constant value, $2\Theta_\infty$, far downstream of the section, where Θ_∞ is a direct measure of the profile drag of the section (*see*, e.g. Refs. 1, 2). Thus

$$\Theta_\infty = \frac{c}{4} C_D, \tag{3.1}$$

where C_D is the drag coefficient based on the chord, c, of the aerofoil.

Once the pressure distribution round the section is known as a function of the base pressure (from the solution of the external flow) the profile drag can be estimated in terms of the base pressure. The profile drag can be calculated in the conventional way by a pressure integral over the aerofoil and an integration of the computed skin-friction values over the wetted surface. But an alternative approach is suggested which is particularly convenient in the present work. This is to express the profile drag as the sum of a pressure integral round a circuit, C, coincident with the upstream *displacement surface*, and a quantity which represents directly the momentum deficit in the boundary layers at separation (Fig. 4). Thus

$$C_D = 4 \frac{\rho_0 u_0^2}{\rho_\infty u_\infty^2} \frac{\theta_0}{c} - \oint C_p d\left(\frac{\Delta^*}{c}\right), \tag{3.2}$$

where $\Delta^*(x)$ is the local ordinate of the displacement surface, suffix $_0$ denotes conditions at the trailing edge, and the other symbols have their usual meanings. This subdivision of the profile drag is similar to that discussed by Cooke in Ref. 24. A formal proof of equation (3.2) is given in the Appendix.

The solution for C_D is rendered determinate by an examination of the changes of momentum thickness which occur along the course of the wake. At the trailing edge the momentum thickness is governed directly by the boundary-layer conditions at separation. The pressure distribution along the wake must therefore be appropriate to the development of the wake from this momentum thickness to a value, $2\Theta_\infty$, far downstream which is compatible with the drag according to equation (3.1). The wake development is expressed analytically by an integration, along the wake, of the

momentum-integral equation applied, not to the whole flow since this integration is implicit in equation (3.2) (*see* Appendix), but to the part of the flow which is orientated throughout in the stream direction. Thus the recirculating flow in the separated region is omitted from consideration and the integral taken over the part of the wake outboard of the dividing streamline.

It is shown that by making certain simplifying assumptions the integration of the momentum equation reduces to a functional relation between C_D (or Θ_∞) and the base pressure. This relation and that derived from the solution of the external flow can then be solved simultaneously to yield the values of profile drag and base pressure (Fig. 5). The latter can subsequently be used to specify the particular pressure distribution round the aerofoil which is consistent with the solution.

4. *The Analysis of the External Flow.*

4.1. Consider an aerofoil section in incompressible flow represented by a source distribution $m_a(x)$ disposed along the x-axis over the interval $-c < x < 0$, the origin lying at the trailing edge (Fig. 6). According to linear theory the source strength can be related to the local slope of the aerofoil contour, i.e.

$$m_a(x) = 2u_\infty \left(\frac{dy}{dx}\right)_{\text{section}} . \tag{4.1}$$

At the trailing edge the source strength is related to the boat-tail angle, $\tan^{-1}\omega$, by

$$m_a(x) = -2u_\infty\omega , \tag{4.2a}$$

and the trailing-edge thickness, h, is given by

$$h = \int_{-c}^{0} \frac{m_a(x)}{u_\infty}\, dx . \tag{4.2b}$$

If the boundary layer is of significant thickness the displacement effect can be taken into account by disposing an additional source distribution, $m_\delta(x)$, along the chordline, such that

$$m_\delta(x) = 2u_\infty \frac{d\delta^*}{dx} , \tag{4.3}$$

where $\delta^*(x)$ is the boundary-layer displacement thickness.

The upstream displacement surface (i.e. that ahead of the trailing edge) is thus represented by the function

$$y = \Delta^*(x)$$

where

$$\begin{aligned} \Delta^* &= y_{\text{section}} + \delta^* \\ &= \int_{-c}^{x} \frac{(m_a + m_\delta)}{2u_\infty}\, dx , \end{aligned} \tag{4.4}$$

for $-c < x < 0$.

In the direct problem the section geometry is known and so m_a can be regarded as given. But, until the surface pressure distribution can be derived, the boundary-layer development cannot be calculated and therefore m_δ is initially unknown. The procedure would be, in practice, to estimate the boundary-layer growth to a first approximation and, on this basis, to derive a first approximation to the pressure distribution. This would allow a second approximation to the boundary-layer growth to be calculated, and so on. It is likely that only a few iterations would be required in most cases. In what follows it will be assumed that m_δ is already known.

The downstream part of the displacement surface (representing the wake) is generated by a further source distribution $m_w(x)$ disposed along the positive x-axis. The local value of Δ^* in the wake (where it is equal to the conventionally defined displacement thickness) is given by

$$\Delta^* = \Delta_0^* + \int_0^x \frac{m_w}{2u_\infty}\, dx, \tag{4.5}$$

where Δ_0^* is the value of Δ^* at $x = 0$, given by

$$\Delta_0^* = \frac{h}{2} + \delta_0^*. \tag{4.5a}$$

At the chordline the combined source distributions, m_a, m_δ and m_w, induce a velocity su_∞ in the stream direction, where s is given by

$$s(x) = \frac{1}{2\pi u_\infty}\left[\int_{-c}^{0} \frac{\{m_a(x') + m_\delta(x')\}\, dx'}{x - x'} + \int_0^\infty \frac{m_w(x')}{x - x'}\, dx'\right], \tag{4.6}$$

taking the Cauchy principal values of the integrals. To the linear approximation the pressure coefficient at a point on the aerofoil is given in terms of the local value of s by

$$C_p = -2s. \tag{4.7a}$$

But it has been pointed out by several authors (Refs. 1, 25, for example) that the linear theory can be improved, particularly near the leading edge, on the basis of a relation between C_p and s which involves the local direction of the velocity vector, i.e.

$$C_p = 1 - \frac{(1+s)^2}{1 + \left(\dfrac{d\Delta^*}{dx}\right)^2}. \tag{4.7b}$$

It has been suggested[38] that equation (4.7b) represents an improvement on equation (4.7a) only forward of the crest of the aerofoil and that the latter should be used aft of the crest. For realistic sections, however, the difference is small and equation (4.7b) will be adopted in the present work for computing the pressure coefficients over the whole section unless otherwise stated.

The foregoing remarks in this section refer explicitly to the incompressible case. The effects of compressibility can be allowed for on the basis of one of the usual 'compressibility laws' discussed in the literature. A suitable one for the purposes of the present work is that of Woods[26], namely

$$C_p = \frac{1}{\beta} C_{pi} - \frac{2}{\beta^2}\left\{1 - \beta + \frac{\gamma + 1}{8}\frac{M^2}{\beta^2}\right\} C_{pi}^2 + 0(C_{pi}^3). \tag{4.8}$$

The equivalent incompressible pressure coefficient, C_{pi}, is related to the induced velocity, s, in the same way as before,

$$C_{pi} = 1 - \frac{(1+s)^2}{1 + \left(\dfrac{d\Delta^*}{dx}\right)^2}. \tag{4.7c}$$

The mixed-boundary-value problem describing the external flow will be formulated on the assumption that the behaviour of the incompressible induced velocity, s, is specified along the initial part of the wake. (To specify C_p would complicate the procedure since $\Delta^*(x)$ is not known at the outset for $x > 0$.) The conditions on the aerofoil surface will be influenced most by the shape of the downstream displacement surface close to the trailing edge—in fact by the part of the displacement surface roughly corresponding to the region of reversed flow. Downstream of the region of confluence the thickness of the wake does not change rapidly with x and it would be

expected that conditions there would have little effect on conditions on the section. Therefore, to simplify the problem it will be assumed that the source distribution, m_w, representing the wake will have vanishing strength for $x > l$, say, where the length l is some measure of the length of the separated region. Equation (4.6) can thus be rewritten as

$$s(x) = s_a(x) + \frac{1}{2\pi u_\infty} \int_0^l \frac{m_w(x')dx'}{x - x'}, \tag{4.9}$$

the top limit of the integral being l instead of infinity. [In equation (4.9) $s_a(x)$ represents the first term on the right-hand side of equation (4.6).] The problem is therefore to determine $m_w(x)$ given that s is specified, equal to $s_w(x)$, say, in the interval $0 < x < l$.

Equation (4.9) can be regarded as an integral equation for m_w to be solved by the standard methods. The solution is given formally by Refs. 27 and 28.

$$\frac{m_w}{2u_\infty} = -\frac{1}{\pi\{x(l-x)\}^{1/2}} \left[K + \int_0^l \frac{\{x'(l-x')\}^{1/2}\{s_w(x') - s_a(x')\}\,dx'}{x - x'} \right], \tag{4.10}$$

where the constant K is chosen to suppress the singularity in m_w at the origin.

In general the integral in equation (4.10) is difficult to evaluate for arbitrary s_w and s_a; but it will be instructive to examine a particular solution, namely, for the restricted case of $s_a = 0$ and s_w = constant. This could represent a cavitation bubble behind a semi-infinite parallel-sided section immersed in a flow of liquid. Under these conditions the value of K is given by

$$K = \frac{\pi}{2} s_w l$$

and the required source distribution, m_w, by

$$\frac{m_w}{2u_\infty} = -s_w \left(\frac{x}{l-x}\right)^{1/2}. \tag{4.11}$$

Alternatively, the right-hand side of equation (4.11) can be expanded in a series to give

$$\frac{m_w}{2u_\infty} = -s_w \left(\frac{x}{l}\right)^{1/2} \left\{ 1 + \frac{1}{2}\left(\frac{x}{l}\right) + \frac{1.3}{2.4}\left(\frac{x}{l}\right)^2 + \frac{1.3.5}{2.4.6}\left(\frac{x}{l}\right)^3 + \ldots \right\}. \tag{4.12}$$

The form of equation (4.12) suggests that for wake pressure distributions which contain a region of roughly constant pressure but which are not exactly equivalent to constant s_w (and $s_a = 0$), the expression for the source distribution, m_w, might be suitably generalised to the form

$$\frac{m_w}{2u_\infty} = \left(\frac{x}{l}\right)^{1/2} \sum_{n=0}^{m} A_n \left(\frac{x}{l}\right)^n. \tag{4.13a}$$

Equation (4.13a) is, however, only suitable for cases where the displacement surface has zero slope and zero curvature immediately upstream of the separation point. If these conditions are not satisfied the expression for m_w must be of the form

$$\frac{m_w}{2u_\infty} = \left(\frac{x}{l}\right)^{1/2} \sum_{n=0}^{m} A_n \left(\frac{x}{l}\right)^n - (\omega' + \omega'' x) \tag{4.13b}$$

where

$$\left.\begin{aligned} \omega' &= -\left(\frac{d\Delta^*}{dx}\right)_{x=-0} \\ \omega'' &= -\left(\frac{d^2\Delta^*}{dx^2}\right)_{x=-0} \end{aligned}\right\}. \tag{4.14}$$

The inclusion of the constant in equation (4.13b) is necessary to suppress a singularity in s at the origin, and the term in x to suppress a singularity in ds/dx for $x = +0$ (ds/dx is generally singular for $x = -0$ but since s is specified only for $x > 0$ this is immaterial). If the boundary-layer thickness at the trailing edge is negligible, ω' will be equal to ω, the tangent of the boat-tail angle. In that case also, ω'' will be zero for many typical aerofoils.

It will be recognised that the term in $(x/l)^{1/2}$ in equation (4.14) implies that the curvature of the displacement surface is infinite for $x = +0$ unless $A_0 = 0$. A_0 will, in general, be non-zero but the singularity is not an embarrassment. Such a behaviour at the separation point is typical of 'free-streamline' models.

The induced velocity arising from the source distributions m_a, m_δ and m_w is given by equations (4.9) and (4.13b):

$$s(x) = s_a(x) + \frac{1}{\pi}\left\{\omega' l - (\omega' + \omega'' x)\log\left|\frac{x}{l-x}\right|\right\} + \\ + \frac{1}{\pi}\int_0^l \left(\frac{x'}{l}\right) \sum_{n=0}^{m}{}' A_n \left(\frac{x'}{l}\right) \frac{dx'}{x - x'}. \tag{4.15}$$

It will be convenient to group the induced velocity, s_a, due to the upstream displacement surface together with the terms in that due to the wake which do not involve the coefficients A_n. Thus, equation (4.15) is written in the form

$$s(x) = \bar{s}_a(x) + \frac{2}{\pi}\sum_{n=0}^{m} A_n I_n\left(\frac{x}{l}\right). \tag{4.16}$$

It will be noted that $\bar{s}_a(x)$ is the induced velocity due to the upstream displacement surface together with a rearward 'extension' of quadratic form

$$\Delta^* = \Delta_0^* - \left(\omega' x + \frac{\omega'' x^2}{2}\right) \tag{4.17}$$

and length l. The surface slope and first derivative of slope are continuous at the junction between the upstream displacement surface and the quadratic component of the downstream displacement surface. For this reason both $\bar{s}_a(0)$ and $(d\bar{s}_a/dx)_{x=0}$ are finite, although, in general, $s_a(0)$ and $ds_a/dx)_{x=0}$ are singular.

The integrals in equation (4.15) have been written as functions of x/l in equation (4.16):

$$I_n\left(\frac{x}{l}\right) = \int_0^l \left(\frac{x'}{l}\right)^{(2n+1)/2} \frac{dx'}{x - x'}. \tag{4.18a}$$

The functions I_n can be evaluated explicitly and are conveniently expressed in the form

$$I_n = I_0\left(\frac{x}{l}\right)^n - \frac{1}{3}\left(\frac{x}{l}\right)^{n-1} - \frac{1}{5}\left(\frac{x}{l}\right)^{n-2} - \ldots\ldots - \frac{1}{2n+1}, \tag{4.18b}$$

with

$$\left.\begin{aligned} I_0 &= \left(-\frac{x}{l}\right)^{1/2}\cot^{-1}\left(-\frac{x}{l}\right)^{1/2} - 1, && \text{for} \quad x < 0 \\ &= \left(\frac{x}{l}\right)^{1/2}\tanh^{-1}\left(\frac{x}{l}\right)^{1/2} - 1, && \text{for} \quad 0 < x < l \\ &= \left(\frac{x}{l}\right)^{1/2}\coth^{-1}\left(\frac{x}{l}\right)^{1/2} - 1, && \text{for} \quad x > l \end{aligned}\right\}. \tag{4.18c}$$

The functions I_0, I_1 and I_2 are tabulated in Table 1 for values of x/l between -5 and 1.

At $x = 0$ the value of s becomes {from equation (4.16)}

$$s(0) = \bar{s}_a(0) - \frac{2}{\pi} \sum_{n=0}^{m} \frac{A_n}{2n+1}, \tag{4.19a}$$

and $s(0)$ is related to the base-pressure coefficient by

$$(C_{pb})_i = 1 - \frac{\{1 + s(0)\}^2}{1 + \omega'^2} \tag{4.19b}$$

together with equation (4.8).

4.2. It will now be necessary to consider the details of the downstream displacement surface (representing the separated region). Equation (4.13b) contains $m + 1$ disposable coefficients, A_n, and an equal number of conditions are required to specify them. Of these conditions, one is furnished by geometric compatibility in the wake, and the remainder can relate to the pressure distribution to be imposed on the wake.

The geometric compatibility condition arises from equation (4.5). If Δ_l^* is the value of Δ^* at $x = l$

$$\begin{aligned} \Delta_0^* - \Delta_l^* &= -\int_0^l \frac{m_w}{2u_\infty} dx \\ &= -2l \sum_{n=0}^{m} \frac{A_n}{2n+3} + \omega' l + \frac{\omega'' l^2}{2}. \end{aligned} \tag{4.20}$$

The approximation that was made that $m_w \approx 0$ for $x > l$ does not necessarily imply that

$$\int_l^\infty m_w dx = 0$$

and that

$$\Delta_l^* = \Delta_\infty^*.$$

If this were so, Δ_l^* could be related to Θ_∞ by means of an appropriate wake shape factor. But there is no apparent reason for equating Δ_l^* to Δ_∞^* and the present calculations have been made on the assumption that

$$\Delta_0^* - \Delta_l = h/2, \tag{4.21}$$

which takes account of the most important contribution to Δ_l^*. Equation (4.21) implies that the wake displacement thickness at $x = l$ is equal to the boundary-layer displacement thickness at separation. The difference in the computed value of C_D due to equating Δ_l^* to $\Delta_0^* - \frac{1}{2}h$ rather than to Δ_∞^* does not appear to be large, amounting to a few percent when the boundary-layer thickness at separation is zero. Since this is a matter on which future work will probably give guidance, Δ_l^* will be left in the analysis as it stands.

Thus m conditions remain to be imposed on equation (4.13) to determine the coefficients A_n, and these will be determined from a consideration of the pressure distribution (or, more correctly, the s_w distribution) along the wake. It will be recalled that the main purpose of the analysis of the external flow is the derivation of the pressure distribution over the aerofoil surface. Therefore the wake pressure distribution must be defined fairly precisely close to the separation point where it will have most influence on the pressures on the aerofoil. Further downstream in the wake the details would appear to be rather less important. The essential features of the wake pressure distribution will be established from an examination of the pressure distribution through a typical

region of separation, i.e. that downstream of a rectangular backward-facing step. The equivalence between the flow past the step and that in the wake of the aerofoil is to be regarded as one of the basic assumptions of the present method.

For a rectangular step in an otherwise plane boundary, an elementary similarity form of the pressure distribution could be constructed on the basis of a relation between

$$\frac{s(x)}{s(0)} \quad \text{and} \quad \frac{s(0)x}{\Delta_0^* - \Delta_l^*}. \tag{4.22}$$

This would be consistent with the assumption that the displacement surface representing the separated region is of a particular geometry and that variations from one condition to another are accommodated by nothing more than changes of scale in the Cartesian directions. Experimental results do, in fact, confirm this assumption in broad terms and a correlation of the data of Ref. 29 on this basis is shown in Fig. 7†. The scatter is considerable but not too great to obscure the general trend of the results, and this correlation should provide an adequate indication of the form of the pressure distribution to be expected in more general cases.

For a rectangular step in an infinite wall ω and $s_a(x)$ are both zero, and if the boundary layer is not too thick ω' and ω'' can be neglected. Thus $\bar{s}_a(x)$ is effectively zero, and the incompressible induced velocity in the neighbourhood of the step is given by equation (4.16a):

$$s(x) = \frac{2}{\pi} \sum_{n=0}^{m} A_n I_n \left(\frac{x}{l}\right) \tag{4.23a}$$

and at separation

$$s(0) = \frac{2}{\pi} \sum_{n=0}^{m} \frac{A_n}{2n+1}. \tag{4.23b}$$

Hence, with the condition of geometric compatibility {equation (4.20)} satisfied

$$\frac{s(x)}{s(0)} = \frac{\sum_{n=0}^{m} A_n I_n \left(\frac{x}{l}\right)}{\sum \frac{A_n}{2n+1}} \tag{4.24a}$$

and

$$\frac{s(0)x}{\Delta_0^* - \Delta_l^*} = \frac{1}{\pi} \frac{\sum_{n=0}^{m} \frac{A_n}{2n+1}}{\sum_{n=0}^{m} \frac{A_n}{2n+3}} \frac{x}{l}. \tag{4.24b}$$

Equations (4.24a) and (4.24b) thus represent an analytical 'pressure' distribution due to a rectangular step, and contain m disposable constants. It will now be the intention to fit this distribution to the experimental correlation in Fig. 7.

---

† The model used in these experiments was similar to the step model described in Ref. 6, but the step height was variable from about $1\frac{1}{2}$ times to 5 times the boundary-layer thickness. Data obtained over a Mach number range of 0·4 to 0·8 are included in the correlation.

The values of s were derived using equations (4.8) and (4.7c). Since the shape of the displacement surface was unknown, however, the term $(d\Delta^*/dx)^2$ in equation (4.7c) was neglected. $d\Delta^*/dx$ was, of course, nearly zero at separation (since the step was rectangular) and was unlikely to be large further downstream.

The form of equation (4.23a) is such that unless

$$\sum_{n=0}^{m} A_n = 0 \tag{4.25}$$

s is logarithmically singular at $x = l$. In practice, in view of equation (4.20), the summation in equation (4.25) is usually negative and $s \to -\infty$ at $x = l$ indicating the presence of a stagnation point (cf. the trailing-edge singularity in classical aerofoil theory). This behaviour can be usefully exploited if the singularity can be identified with the overshoot in the pressure distribution. If this is done it is then necessary to impose only two further conditions to define a function $s(x)$ which exhibits the same trends as the data in Fig. 7. These are

$$\left.\begin{aligned} &\text{(i)} && \left(\frac{ds}{dx}\right)_{x=+0} = 0 \\ &\text{(ii)} && (s)_{x=l/2} = s(0) \end{aligned}\right\} \tag{4.26}$$

Equations (4.26) ensure that s is essentially constant over the initial part of the separation bubble.

Thus m in equation (4.13b) can be taken as 2 and the values of the three coefficients A_0, A_1 and A_2 are given by equations (4.20), (4.23a), (4.23b) and (4.26) which, together with the definitions of the functions I_n (equations (4.18)), lead to the matrix equation

$$[M_1][A_n] = [M_2], \tag{4.27}$$

where

$$[M_1] = \begin{bmatrix} 1 & -1 & -\frac{1}{3} \\ \frac{1}{3} & \frac{1}{5} & \frac{1}{7} \\ 1 + I_0\left(\frac{1}{2}\right) & \frac{1}{3} + I_1\left(\frac{1}{2}\right) & \frac{1}{5} + I_2\left(\frac{1}{2}\right) \end{bmatrix}$$

$$[M_2] = \begin{bmatrix} 0 \\ -\dfrac{(\Delta_0^* - \Delta_l^*)}{2l} \\ 0 \end{bmatrix},$$

and $[A_n]$ is a column matrix of the coefficients A_0, A_1 and A_2. The function $s(x)$ defined by equations (4.23a) and (4.27) is shown, in the similarity form {equations (4.24)}, in Fig. 7 along with the experimental data. When further experimental results are available, it may be possible to revise the criteria {equations (4.26)} for determining the coefficients A_n but at present it would seem that there is little possibility of improvement. By retaining more terms in the expansion for m_w {equation (4.13b)} the singularity in s at $x = l$ could be suppressed, but then further restrictions on s would need to be imposed and this would tend to limit the generality of application. In their present form equations (4.26) are sufficient to define the behaviour of the function $s(x)$ without unduly restricting its generality.

4.3. In the general case when ω', ω'' and $s_a(x)$ do not vanish [i.e. when $\bar{s}_a(x)$ is non-zero] the similarity form of the wake 'pressure' distribution is no longer valid. Nevertheless it will be assumed

that the general form of the distribution is the same as that illustrated in Fig. 7 and that the criteria stated in equations (4.26) can still be invoked. Hence, taking $m = 2$ as before, the condition that equations (4.20) and (4.26) be satisfied leads to the matrix equation

$$[M_1][A_n] = [M_3], \tag{4.28}$$

where $[M_1]$ and $[A_n]$ retain their definitions as in equation (4.27) and $[M_3]$ is a column matrix defined by

$$[M_3] = \begin{bmatrix} -\dfrac{\pi l}{2}\left(\dfrac{d\bar{s}_a}{dx}\right)_{x=+0} \\ \tfrac{1}{2}\left\{\omega' + \dfrac{\omega'' l}{2} - \dfrac{\Delta_0^* - \Delta_l^*}{l}\right\} \\ \dfrac{\pi}{2}\left\{\bar{s}_a(0) - \bar{s}_a\left(\dfrac{l}{2}\right)\right\} \end{bmatrix}.$$

It will be noted that $[M_3]$ reduces to $[M_2]$ if $\omega' = \omega'' = 0$ and $\bar{s}_a \equiv 0$.

4.4. Equation (4.28) effectively completes the solution of the external inviscid flow. The coefficients, A_n, are determined in terms of the section geometry and the length, l, of the separated region. The induced velocity over the aerofoil is thus given as a function of l by

$$s(x) = \bar{s}_a(x) + \frac{2}{\pi}\left\{A_0 I_0\left(\frac{x}{l}\right) + A_1 I_1\left(\frac{x}{l}\right) + A_2 I_2\left(\frac{x}{l}\right)\right\} \tag{4.29a}$$

with [equations (4.15) and (4.16)]

$$\bar{s}_a(x) = s_a(x) + \frac{1}{\pi}\left\{\omega'' l - (\omega' + \omega'' x)\log\left|\frac{x}{l-x}\right|\right\}. \tag{4.29b}$$

The length l can, in turn, be related uniquely to the value of $s(0)$, since

$$s(0) = \bar{s}_a(0) - \frac{2}{\pi}\left(A_0 + \frac{A_1}{3} + \frac{A_2}{5}\right) \tag{4.30}$$

and $\bar{s}_a(0)$ is a function of l as is seen from equation (4.29b).

Hence, using equations (4.19b) and (4.8), the pressure distribution over the aerofoil (or the upstream displacement surface) can be expressed as a singly infinite family of solutions, each corresponding to a particular value of the base pressure. For a range of values of C_{pb} the pressure distribution can be computed and the profile drag derived, using either equation (3.2) or the more conventional method. Thus, from an analysis of the external flow, one relation between C_D and C_{pb} is established. A second such relation will now be derived from a consideration of the turbulent flow in the wake.

5. *The Analysis of the Wake.*

5.1. Consider the flow in one half of the wake outboard of the dividing streamline ψ_D. [For the purposes of the present discussion ψ_D will be taken to denote the streamline linking the separation point and the point of confluence (Fig. 3), and also its extension downstream along the wake centre

line (Fig. 8)]. Thus the recirculating flow in the separation bubble is omitted from consideration. Let θ be the momentum thickness of the part of the viscous layer between ψ_D and the external stream, i.e.

$$\rho u\theta = \int_{\psi_D}^{\infty} (1-u^*)d\psi \tag{5.1}$$

where

$$\psi = \int \rho u \, dy . \tag{5.2}$$

The momentum thickness θ varies from θ_0 at the separation point to Θ_∞ far downstream.

The momentum-integral equation[43] can be applied to the part of the wake under consideration,

$$\frac{d\theta}{dx} + \theta(H+2-M^2)\frac{1}{u}\frac{du}{dx} = \frac{\tau}{\rho u^2}, \tag{5.3}$$

where θ is defined as in equation (5.1) and H is the appropriate shape factor†. It may be verified that the momentum-integral equation retains its usual form even though the velocity on ψ_D is non-zero. The shear stress τ acts along the dividing streamline between the separation point, S, and the point of confluence, R (Fig. 8). Downstream of R the shear stress vanishes on account of the symmetry of the wake. The distance SR will be denoted by l'.

The momentum-integral equation may be formally integrated along the wake from S to infinity to give

$$\Lambda_\infty\Theta_\infty = \Lambda_0\theta_0 + \int_0^{l'} \frac{\Lambda\tau}{\rho u^2}\, dx \tag{5.4a}$$

where the integrating factor Λ is defined by

$$\log \Lambda = \int (H+2-M^2)\frac{du}{u}, \tag{5.4b}$$

there being no contribution to the integral in equation (5.4a) for $x > l'$ since the shear stress is zero.

In general the evaluation of the integrating factor would require a knowledge of the variation of H and u along the wake. However, H plays only a secondary rôle in equation (5.4b) and little accuracy will be lost if H is regarded as a function of Mach number alone. For unit Prandtl number and zero heat transfer the shape factor H can be related to an equivalent shape factor H_i in incompressible flow by the expression[31]

$$H = (H_i+1)\frac{T_t}{T} - 1, \tag{5.5}$$

where T and T_t are the static and total temperatures, respectively, appropriate to the Mach number M at the edge of the wake. In the context of the present problem H_i varies between extremes of 2 to $2\frac{1}{2}$ at the point of confluence (i.e. equal to a typical separation value), and unity far downstream. At the separation point the value of H_i is about 1·2 to 1·4, depending on Reynolds number, and in the free-shear layer approximately the same. Hence it will be reasonable to give H_i a mean value of about 1·5.

---

† In equation (5.3) x is, strictly speaking to be measured along the dividing streamline. For moderate boat-tail angles and typical values of C_{pb} there is, however, little loss of accuracy by taking x as the projection of this distance on the wake centre line.

Thus, if H_i is considered constant equations (5.4b) and (5.5) give

$$\frac{\Lambda}{\Lambda_\infty} = \left(\frac{M}{M_\infty}\right)^{H_i+2} \left(\frac{T}{T_\infty}\right)^{(\gamma+1)/2(\gamma-1)}. \tag{5.6}$$

The evaluation of the integral in equation (5.4a) in an approximate form is not difficult. The pressure distribution between the points S and R (Fig. 8) can be idealised into a region of constant pressure followed by an abrupt pressure rise. Thus, if the pressure is assumed to start to rise at $x = l''$, the integral can be written

$$\int_0^{l'} \frac{\Lambda\tau}{\rho u^2}\, dx = \frac{\Lambda_0}{\rho_0 u_0{}^2} \int_0^{l'} \bar{\tau}\, dx + \int_{l''}^{l'} \left(\frac{\Lambda\tau}{\rho u^2} - \frac{\Lambda_0\bar{\tau}}{\rho_0 u_0{}^2}\right) dx, \tag{5.7}$$

where $\bar{\tau}(x)$ is the variation of τ with x corresponding to the development of the shear layer at constant pressure. The essential point of the approximation to be made is that, if the pressure rise is sufficiently abrupt, $l'' \to l'$, and the second term on the right-hand side of equation (5.7) is small compared with the sum of the first term and the quantity $\Lambda_0\theta_0$ which appears in equation (5.4a). Thus, to a first approximation, equation (5.4a) becomes

$$\Lambda_\infty\Theta_\infty = \Lambda_0\theta_0 + \frac{\Lambda_0}{\rho_0 u_0{}^2} \int_0^{l'} \bar{\tau}\, dx. \tag{5.8}$$

The integral involving $\bar{\tau}$ can be evaluated from the momentum-integral equation appropriate to the condition of constant pressure, i.e.

$$\frac{d\theta}{dx} = \frac{\bar{\tau}}{\rho_0 u_0{}^2},$$

$$\int_0^{l} \bar{\tau}\, dx = \rho_0 u_0{}^2(\hat{\theta} - \theta_0), \tag{5.9}$$

say. The quantity $\hat{\theta}$ in equation (5.9) is interpreted as being the value which the momentum thickness θ [as defined in equation (5.1)] would reach if the shear layer developed over a length l' at a constant pressure equal to the base pressure. The asymptotic momentum thickness of the wake is thus given by equations (5.8) and (5.9):

$$\Theta_\infty = \frac{\Lambda_0}{\Lambda_\infty}\,\hat{\theta}. \tag{5.10}$$

In incompressible flow the quantity Λ {equation (5.6)} reduces to a power of the velocity at the edge of the wake and equation (5.10) can then be written

$$\Theta_\infty = \left(\frac{u_0}{u_\infty}\right)^{H_i+2} \hat{\theta}. \tag{5.11a}$$

It may be noted that if the trailing-edge thickness of the aerofoil tends to zero, l' also tends to zero and $\hat{\theta}$ is equal to θ_0 {*see* e.g. equation (5.9)}. In this case equation (5.11a) reduces to

$$\Theta_\infty = \left(\frac{u_0}{u_\infty}\right)^{H_i+2} \theta_0, \tag{5.11b}$$

which is of the same form as the wake solution given by Squire and Young[30] for the sharp-trailing-edge aerofoil, H_i being, as in the present work, a mean value along the wake. Similarly, equation (5.10), with $\hat{\theta}$ replaced by θ_0, forms the basis of the method of Ref. 37 for the prediction of the profile drag of conventional aerofoils in compressible subsonic flow.

5.2. The value of $\hat{\theta}$ can be readily determined, as a function of the momentum thickness of the boundary layer at separation and the distance, l', from the separation point, if it can be assumed that the flow in the outer part of the shear layer is not significantly influenced by the presence of the other shear layer and the reversed flow in the separated region. In this case the shear layer can be regarded as equivalent to that generated by the mixing of a stream with a quarter-infinite fluid at rest. Some calculations have been made of the variation of $\hat{\theta}$ with θ_0 and l' for incompressible flow and the results are presented in Fig. 9. The calculations were based on the theoretical velocity profile of Tollmien for the case of the shear layer growing from zero thickness, together with the approximate method of Kirk[23, 32] for dealing with the effect of the initial boundary layer†. Also shown in Fig. 9 is the variation of the velocity ratio, $u_D{}^*$, on the dividing streamline with θ_0 and l'. The results involve the constant σ which relates to the rate of spread of the asymptotic layer (i.e. the layer developing from zero thickness at separation). The measured value of σ is about 12 at low speeds.

The derivation of equivalent data for Mach numbers other than zero must depend on some assumption concerning the effect of compressibility on the development of the asymptotic free-shear layer. It has been established experimentally that the rate of spread of the turbulent shear layer is smaller at supersonic speeds than in incompressible flow (although the published data on the associated increase of σ with Mach number is far from coherent). At subsonic speeds, however, the most reliable evidence[39, 40] suggests that there is little increase of σ above the level appropriate to zero Mach number. Similarly, the shape of the velocity profile could be expected to be substantially unaltered from its low-speed form. Thus there can be some confidence that the data illustrated in Fig. 9 will be approximately valid throughout the subsonic speed range. The calculations in the present work have been based on this assumption.

5.3. It remains to attach some value to the effective length, l', of the free-shear layer. In general l' will not be equal to the length, l, of the source distribution representing the separated region in the analysis of the external flow (*see* Section 4, above). In fact, experience has shown that l' is usually equal to about $0{\cdot}9\ l$ or $0{\cdot}95\ l$ depending on conditions. Values of this order could be used as a first approximation.

More precisely l' may be determined in a particular case from a consideration of the acceleration and subsequent retardation of the fluid on the dividing streamline in the free-shear layer. If the compression up to the point of confluence can be regarded as quasi-isentropic the pressure rise may be related to the velocity ratio $u_D{}^*$ by

$$\frac{p_r}{p_b} = \left[\frac{1 + \frac{\gamma - 1}{2} M_0{}^2}{1 + \frac{\gamma - 1}{2} M_0{}^2 (1 - u_D{}^{*2})} \right]^{\gamma/(\gamma-1)}, \tag{5.12a}$$

where p_r is the pressure at the point of confluence; or if the Mach number is small

$$C_{pr} - C_{pb} = (1 - C_{pb}) u_D{}^{*2} + 0(M_\infty{}^4). \tag{5.12b}$$

† Recent work by McDonald and Acklam[41] has shown that values of $\hat{\theta}$ calculated using Kirk's approximation and the error-function velocity profile are indistinguishable from values calculated using the theory of Ref. 32. Thus, there seems to be considerable justification for using Kirk's approximation together with the more accurate velocity profile of Tollmien.

Either of these equations, together with values of u_D^* from Fig. 9, represents a relation between C_{pb}, C_{pr} and l', since θ_0 can be considered known. A second relation between these quantities is furnished by the analytic wake pressure distribution derived as part of the analysis of the external flow. Thus for particular values of θ_0 and C_{pb} a wake pressure distribution is specified and it is a simple matter to find the point on it where the pressure coefficient is equal to C_{pr} as given by equation (5.12a) or (5.12b). Since the pressure rise through the region of confluence is abrupt the derived value of l' is insensitive to small errors in C_{pr} and equation (5.12b) can probably be used without significant loss of accuracy throughout the speed range under consideration.

5.4. This completes the analysis of the wake. The variation of l' with base-pressure coefficient is obtained, as described in Section 5.3, from the analysis of the external flow appropriate to the particular aerofoil being considered. For each value of C_{pb}, and the given value of θ_0, the value of $\hat{\theta}$ is determined from the data in Fig. 9. The wake momentum thickness at infinity (and hence C_D) is then given by equation (5.10), the ratio Λ_0/Λ_∞ being a function only of C_{pb} and the Mach number. Thus the analysis of the wake yields a second relation connecting the profile drag coefficient and the base-pressure coefficient. This relation and the one derived from the analysis of the external flow can then be solved simultaneously to give C_D and C_{pb} (*see* Fig. 5).

6. *Some Computed Results.*

6.1. *Semi-Infinite Parallel-Sided Section.*

This is the most elementary example of a blunt-trailing-edge section and can be considered to illustrate the effect of the boundary-layer thickness on base pressure, and also the variation of the latter with Mach number.

The asymptotic wake momentum thickness is given by equations (3.1) and (3.2):

$$\Theta_\infty = \frac{\rho_0 u_0^2}{\rho_\infty u_\infty^2}\,\theta_0 - \frac{h + 2\delta_0^*}{4}\,C_{pb} \tag{6.1}$$

the pressure integral in equation (3.2) reducing to the trivial product of the base-pressure coefficient and the total thickness of the displacement surface at the trailing edge. If H_0 is the shape factor of the boundary layer at separation, equation (6.1) may be written

$$\frac{\Theta_\infty}{h} = \left(\frac{\rho_0 u_0^2}{\rho_\infty u_\infty^2} - \frac{H_0}{2}\,C_{pb}\right)\frac{\theta_0}{h} - \frac{1}{4}\,C_{pb}. \tag{6.2}$$

The matrix equation for the coefficients A_n defining the source distribution which represents the separated region is as given in equation (4.27), $\Delta_0^* - \Delta_l^*$ being taken as $\frac{1}{2}\,h$.

The viscous solution is represented by equation (5.8) with values of $\hat{\theta}$ derived from Fig. 9. The values of l', the effective length of the shear layer were obtained in the calculations by the method suggested in Section 5.3.

The predicted base-pressure coefficients are presented in Fig. 10, C_{pb} being shown as a function of the ratio, h/θ_0, of the trailing-edge thickness to the momentum thickness of the boundary layer at separation. Calculations were made for Mach numbers of 0, 0·4, 0·6 and 0·8. Also shown in Fig. 10 are the results of base-pressure measurements on backward-facing steps. It is seen that, although there is some deviation the theory accords well with the experimental results. In particular the insensitivity of the base pressure to changes of trailing-edge thickness, for values of h/θ_0 greater than about 20, is reproduced—and indeed exaggerated—by the theory. For small values of h/θ_0 the validity of some of the details of the analysis becomes increasingly questionable, and the agreement

between the predicted values and the measurements by Wieghardt is certainly as good as could be expected. For a more critical assessment of the accuracy of the method, more reliable experimental data are urgently required over the whole range of conditions.

The variation of base-pressure coefficient with Mach number indicated by the theory is shown in Fig. 11 in comparison with the measurements of Ref. 29. The agreement is again satisfactory and there is reason to suggest that the small discrepancies might be attributed as much to inadequacies in the test conditions as to those in the analysis. When sonic velocity is reached locally at the trailing edge the theory ceases to be valid. This is chiefly a result of the interruption of the direct relationship between the drag and the asymptotic momentum thickness of the wake. When regions of supersonic flow exist in the flow-field wave drag is generated which is not accounted for in the momentum deficit of the wake as such. An examination of the present solution indicates that as Θ_∞ represents a progressively smaller fraction of the total drag of the section the base pressure falls. This behaviour is qualitatively consistent with the observed variation of base pressure at transonic speeds.

It might be thought that the comparison between theory and experiment in Figs. 10 and 11 is not a valid one since empirical data from the same experiments are already used in the analysis. However this is not so. For the simple case of a semi-infinite, parallel-sided section the analysis of the external flow, which contains the empirical information, plays a trivial rôle, entering only *via* the relation between l' and C_{pb}. This relation could easily have been obtained by some other means, for instance, by assuming that the separated region could be represented by a parabola as far as the external flow is concerned.

6.2. *Semi-Infinite Parallel-Sided Section with Boat-Tailing.*

We now consider the flow past a semi-infinite, parallel-sided section with a truncated-wedge afterbody. This is a somewhat artificial example in so far as, in a real flow, boundary-layer separation would be likely to occur at the shoulder of the section where there is a discontinuity of surface slope. Nevertheless it will serve to demonstrate the extent to which base drag can be reduced by modification of the section geometry. To simplify the analysis it will be assumed that the boundary-layer thickness at the trailing edge is zero, and the calculations will be performed for incompressible flow.

The source distribution representing the afterbody, which will be assumed to be of length l_a, can be written

$$m_a(x) = -2u_\infty\omega, \tag{6.3}$$

where $(\tan^{-1}\omega)$ is the boat-tail angle, and will be disposed over the interval $-l_a \leqslant x < 0$. The induced velocity $\bar{s}_a$ (equation (4.16), due to the afterbody and the constant component, $-2u_\infty\omega$, of the source distribution representing the initial part of the wake, is given by

$$\bar{s}_a = -\frac{\omega}{\pi}\log\left|\frac{x+l_a}{l-x}\right|, \tag{6.4}$$

and the column matrix $[M_3]$, (equation (4.28)), becomes

$$\frac{\omega}{2}\begin{bmatrix} 1-\dfrac{h}{2\omega l} \\ \dfrac{l}{l_a}+1 \\ \log\left(\dfrac{l}{l_a}+2\right) \end{bmatrix}. \tag{6.5}$$

The coefficients A_0, A_1 and A_2, defining the non-linear component of the source distribution representing the separated region, are thus determined. For a given value of $s(0)$, the induced velocity field $s(x)$ over the afterbody can then be written in the form

$$s(x) = \frac{\omega}{\pi}\left[\log\left|\frac{l-x}{x+l_a}\right| + \frac{2}{\omega}\left\{A_0 I_0\left(\frac{x}{l}\right) + A_1 I_1\left(\frac{x}{l}\right) + A_2 I_2\left(\frac{x}{l}\right)\right\}\right] \tag{6.6}$$

with l related to $s(0)$ by

$$s(0) = \frac{\omega}{\pi}\left[\log\frac{l}{l_a} - \frac{2}{\omega}\left(A_0 + \frac{A_1}{3} + \frac{A_2}{5}\right)\right]. \tag{6.7}$$

The pressure distribution over the afterbody can be derived from the induced velocities using equation (4.7b), which reduces to

$$C_p = 1 - \frac{\{1+s(x)\}^2}{1+\omega^2}. \tag{6.8}$$

The drag is then given by an integration of the pressures over the section. If $\bar{C}_D$ is the drag coefficient based on the maximum thickness of the section,

$$\bar{C}_D = -\frac{1}{t}\left\{hC_{pb} - 2\omega\int_{-l_a}^{0} C_p\,dx\right\}. \tag{6.9}$$

In the present calculations equation (6.8) was linearised to the approximate form

$$C_p = -2s(x), \tag{6.10}$$

yielding a pressure distribution which is readily integrable analytically. Thus

$$\bar{C}_D = \frac{2}{t}\left\{hs(0) - 2\omega\int_{-l_a}^{0} s\,dx\right\}, \tag{6.11}$$

$$\int_{-l_a}^{0} s\,dx = \frac{\omega l_a}{\pi}\left[\left(1+\frac{h}{2\omega l_a}\right)\log\left(1+\frac{l}{l_a}\right) - \frac{h}{2\omega l_a}\log\frac{l}{l_a} + \right.$$
$$\left. + \frac{4}{\omega}\left\{\frac{A_0}{3}I_0\left(-\frac{l_a}{l}\right) + \frac{A_1}{5}I_1\left(-\frac{l_a}{l}\right) + \frac{A_2}{7}I_2\left(-\frac{l_a}{l}\right)\right\}\right]. \tag{6.12}$$

From geometric considerations t can be expressed in terms of the other section parameters,

$$t = h + 2\omega l_a. \tag{6.13}$$

The drag coefficient of the section can thus be determined as a function of l, and hence of base pressure {equations (4.18b) and (4.8)}, and the asymptotic wake momentum thickness is given by

$$\Theta_\infty = \frac{t}{4}\bar{C}_D. \tag{6.14}$$

The viscous solution [equation (5.10)] takes a simple form in incompressible flow. The ratio Λ_0/Λ_∞ is expressible as a power of the local velocity u_0 at separation, as in equation (5.11a), or, alternatively, as a function of the base-pressure coefficient:

$$\frac{\Lambda_0}{\Lambda_\infty} = \left(\frac{u_0}{u_\infty}\right)^{H_i+2} \tag{6.15}$$

$$= (1-C_{pb})^{(H_i+2)/2}$$

$$= (1-C_{pb})^{7/4}, \tag{6.16}$$

for $H_i = 1{\cdot}5$. Furthermore, since the boundary-layer thickness at separation is zero, the momentum thickness, θ, of the part of the shear layer outboard of the dividing streamline can be expressed in its asymptotic form

$$\frac{\sigma\hat{\theta}}{l'} = 0{\cdot}14, \tag{6.17}$$

the value of the constant being appropriate to the velocity profile of Tollmien. In the present calculations l' was taken equal to $0{\cdot}9\ l$.

Two exercises were carried out to demonstrate the effect of boat-tailing on the base pressure. In the first, the boat-tail angle was held constant at $5{\cdot}71°$ (i.e. for which $\omega = 0{\cdot}1$), and the trailing-edge thickness varied at the expense of allowing the length of the afterbody to vary. The predicted base-pressure coefficient and drag are shown as functions of trailing-edge thickness in Fig. 12. In the second exercise the length of the afterbody was held constant and changes of trailing-edge thickness were accommodated by allowing the boat-tail angle to vary. The results of these calculations are illustrated in Fig. 13.

The results of both exercises are broadly similar, and indicate that useful reductions in drag can be achieved by decreasing the trailing-edge thickness, compared with the maximum thickness of the section by boat-tailing. In the first case the initial rate of reduction in drag is somewhat greater than in the second, and this can be attributed to the fact that for equal values of h/t, near unity, the boat-tail angle is greater in the first case than for the constant-length afterbody. When the value of h/t is reduced to about $0{\cdot}4$ the base-pressure coefficient is observed to become positive. At this condition there is no 'base drag' as such but full pressure recovery does not occur over the afterbody and a net drag remains. In the limit of a sharp trailing edge (i.e. $h = 0$) the calculations indicate zero drag and the presence of a rear stagnation point. This is, of course, a consequence of the assumption of zero boundary-layer thickness at separation.

In practice a wedge afterbody would not be a suitable configuration, and the section would need to be designed as a whole, taking proper account of the boundary-layer growth. On the basis of the present calculations it would seem beneficial, from a drag standpoint, to keep the trailing-edge thickness reasonably small compared with the maximum thickness of the section thus incorporating some degree of boat-tailing. Nevertheless, it cannot be assumed without proof that in any given case the minimum drag is realised when the trailing-edge thickness is precisely zero. Further work is needed to investigate whether, and if so under what conditions, a drag minimum can occur for non-zero trailing-edge thickness.

6.3. *Truncated RAE 103 Section.*

This example is chosen to illustrate the application of the present method to realistic aerofoil shapes. The calculations are again performed for the restricted case of incompressible flow and zero boundary-layer thickness at the trailing edge.

A comparison is made between the characteristics of the basic RAE 103 aerofoil section[34, 35] of 10 per cent thickness-chord ratio and two 10 per cent thick blunt-trailing-edge sections defined as follows: Aerofoil I is derived by the truncation of a 9 per cent thick RAE 103 section at $0{\cdot}9$ chord, Aerofoil II by the truncation of an 8 per cent thick RAE 103 section at $0{\cdot}8$ chord.

The RAE 103 section has a constant surface slope aft of $0{\cdot}787$ chord, and this property allows a simple determination to be made of $\bar{s}_a$ for the truncated sections from the induced velocity distribution, s_B say, appropriate to the basic section from which each is derived. s_B can be computed by

any of the standard methods, that due to Weber[25] being used in the present calculations. Now consider one of the truncated sections whose chord occupies the interval $-c < x < 0$ of the x-axis. The chord of the corresponding basic section is longer and will extend from $x = -c$ to $x = c_B - c$, say. The source distributions representing the basic and truncated sections differ only by the constant component of strength $-2u_\infty\omega$ disposed over the interval $0 < x < (c_B - c)$. But $\bar{s}_a$ is the induced velocity due to the truncated section together with the constant term in the source distribution representing the separated region which extends from the origin to $x = l$. Thus $\bar{s}_a$ will differ from s_B only by the induced velocity due to a constant source distribution of strength $-2u_\infty\omega$ disposed along the x-axis from $x = l$ to $x = c_B - c$, i.e.

$$\bar{s}_a = s_B + \frac{\omega}{\pi}\log\left|\frac{x}{x-(c_B-c)}\right| . \tag{6.18}$$

The terms of the matrix $[M_3]$ in equation (4.28) can thus be determined, and the induced velocity distribution $s(x)$ subsequently derived in terms of the value $s(0)$ at the trailing edge [equations (4.29a), (4.29b) and (4.30)].

In the present example the pressure distribution round the section cannot be integrated analytically, and the precise relation between C_p and s {equation (4.7b)} is used. The computations otherwise proceed as in the previous example (Section 6.2 above).

The chordwise pressure distributions for the RAE 103 section, and Aerofoils I and II, are shown in Fig. 14. The suction on the forward part of Aerofoils I and II is lower than that on the RAE section of 10 per cent thickness-chord ratio, and the 'rooftop' extends to a more rearward chordwise station. This is because the three aerofoils are of equal thickness but the truncated sections have longer basic chords. The pressure distributions on Aerofoils I and II are broadly similar to those of the basic sections from which they were each derived, except close to the trailing edge within the region of influence of conditions on the base. Fig. 15 shows the pressure distributions plotted in terms of the ordinate, y, measured normal to the chordline. This presentation accentuates the difference between the pressures over the rear of the truncated sections and those on the sharp-trailing-edge section. Whereas in the latter case full pressure recovery takes place over the rearward-facing area (a consequence of the assumption of zero boundary-layer thickness), in the former, full recompression is inhibited and the pressure remains constant over the base making an appreciable contribution to the drag.

The base-pressure and drag data can be summarised as follows:

Section	t/c (%)	h/c (%)	C_{pb}	C_D
RAE 103	10	0	—	0
Aerofoil I	10	2·0975	0·0080	0·0026
Aerofoil II	10	4·1950	−0·0822	0·0063

The results confirm the conclusions of Section 6.2 above in that the base pressure on a section truncated well aft of its position of maximum thickness can be substantially higher than that on a section without boat-tailing (for which $C_{pb} \approx -0{\cdot}2$). The values of the drag coefficient, C_D, must, of course, be interpreted in the context of the neglect of the boundary-layer growth on the section. Thus the skin-friction drag has been neglected, and also form drag associated with the displacement

effect of the attached boundary layer. The skin friction drag component is likely to be approximately the same for the three sections, but the form drag increment is likely to decrease the further forward the position of truncation. Since much of the rear pressure recovery on Aerofoils I and II has already been lost the boundary-layer growth would presumably be less than on the basic section and less additional form drag would be developed. Thus, to add to the values of C_D indicated in the table an increment equal to the total drag† of the RAE 103 section would seem to yield pessimistic estimates of the true drag values of the truncated sections.

7. *Concluding Remarks.*

An analysis has been formulated of the subsonic non-periodic flow past a two-dimensional, symmetrical, blunt-trailing-edge aerofoil section at zero incidence. The problem stated is to some extent hypothetical, but is considered to provide a basis for a study of the characteristics of sections of finite trailing-edge thickness when the vortex street has been partially or wholly suppressed. The analysis may also find an application in other problems involving separated flow.

The analysis involves parallel solutions of the external inviscid flow and of the turbulent flow in the wake. The analysis of the external flow, which is a mixed-boundary-value problem, is concerned with the derivation of the surface pressure distribution over the aerofoil as a function of the base pressure. For the purposes of the solution the pressure distribution along the initial part of the wake is specified in general terms by criteria which have been established from an examination of the pressure distributions downstream of rearward-facing steps.

Knowledge of the pressure distribution over the aerofoil in terms of the base pressure permits the computation of the profile drag as a function of base pressure. The solution is subsequently rendered unique by the consideration of compatibility requirements in the wake.

In subsonic flow the momentum thickness, Θ_∞, of the wake at infinity downstream is known in terms of the profile drag of the section. Thus the wake momentum thickness must change from its known value at the trailing edge to Θ_∞ far downstream after negotiating the changes of pressure, along the wake, from the base pressure to freestream static pressure. The wake analysis is based on the work of Squire and Young but is formulated to take into account the region of reversed flow immediately downstream of separation.

The application of the method is illustrated by a number of examples. Computations have been made of the variation, with Mach number and boundary-layer thickness, of the base pressure on a long, parallel-sided section. The results are compared with measurements of the base pressure on rectangular backward-facing steps, and satisfactory agreement is obtained over the range of validity of the theory. The analysis ceases to be valid when local supersonic flow exists at the separation point. This is chiefly a result of the interruption of the direct proportionality between the drag and the asymptotic wake momentum thickness. It is shown that the subsequent relationship between Θ_∞ and the drag would lead to a variation of base pressure with Mach number which is qualitatively consistent with the observed behaviour at transonic speeds.

---

† A computation of the drag of the basic RAE 103 section of 10 per cent thickness-chord ratio was made by the method of Ref. 1, on the assumption of transition at 10 per cent chord. The result was as follows:

$$R_e = 10^6,\ C_D = 0{\cdot}0108$$
$$= 10^7,\quad = 0{\cdot}0065.$$

Calculations have also been made for two further types of configuration for the restricted case of incompressible flow and zero boundary-layer thickness at separation (i.e. for infinite Reynolds number).

The first is a long parallel-sided section to which has been added a truncated-wedge afterbody. The results indicate a rapid increase of base pressure, and a similar decrease of total afterbody drag, as the trailing-edge thickness is reduced below the thickness of the parallel forebody. For a given ratio of trailing-edge thickness to forebody thickness, the base pressure is found to rise with increase of the boat-tail angle. [However, since the boundary-layer growth on the afterbody was omitted from consideration in the calculations, the results do not indicate the maximum usable boat-tail angle which would be determined by incipient separation.]

The second configuration discussed is a truncated aerofoil of RAE 103 section. Calculations have been made of the pressure distribution and profile drag of two blunt-trailing-edge sections of 10 per cent thickness-chord ratio derived, respectively, by the truncation of a 9 per cent thick basic section at 0·9 chord (Aerofoil I), and an 8 per cent thick basic section at 0·8 chord (Aerofoil II). The chordwise pressure distributions (Fig. 14) correspond closely to those of the basic sections from which the aerofoils were derived except towards the trailing edge where the expansion takes place associated with conditions on the base. The base-pressure coefficient on Aerofoil I, which has a trailing-edge thickness of about 2 per cent of the chord, is approximately zero and the drag coefficient equal to 0·0026. On Aerofoil II, with a trailing-edge thickness of about 4 per cent, the base pressure coefficient is about $-0·08$ and the drag coefficient 0·0063. On the assumption of zero boundary-layer thickness, the corresponding drag of a sharp-trailing-edge section would, of course, be zero. In a real case it would be expected that the drag coefficient of the truncated aerofoils would be slightly less than the sum of the values mentioned above and typical values of C_D for the basic 10 per cent thick RAE 103 section, under similar conditions of Reynolds number and transition position.

Acknowledgements.

The author wishes to acknowledge the assistance of Mr. S. Cox and Miss F. M. Worsley with the calculations, and is indebted to Dr. R. C. Lock for useful criticism of this paper.

NOTATION

x, y		Cartesian co-ordinates (origin at trailing edge)
c		Chord
t		Maximum thickness of section
h		Trailing-edge thickness
ω		Tan (boat-tail angle)
l_a		Length of afterbody
l, l'		Length of separated region
u		Velocity
M		Mach number
β	$=$	$(1-M^2)^{1/2}$
γ		Isentropic index
p		Pressure
ρ		Density
T		Temperature
ψ		Stream function $= \rho u \int \rho^* u^* dy$
Re		Reynolds number based on chord
$\theta, \hat{\theta}, \Theta$		Momentum thickness
δ^*, Δ^*		Displacement thickness
H		Shape factor (ratio of displacement to momentum thickness)
σ		Shear-layer parameter (inversely proportional to rate of spread of asymptotic layer)
$\tau, \bar{\tau}$		Shear stress
Λ		Function defined in equation (5.3a)
s		Non-dimensional induced velocity (equivalent to $s^{(1)}$ of Ref. 25)
m		Source strength
A_n		Coefficient in equation (4.14)
I_n		Function defined in equation (4.17)
$[M]$		Matrix

C_p Pressure coefficient

$$= \frac{p - p_\infty}{\frac{1}{2}\rho_\infty {u_\infty}^2}$$

C_D, $\bar{C}_D$ Drag coefficient

$$C_D = \frac{\text{Drag}}{\frac{1}{2}\rho_\infty {u_\infty}^2 c}$$

$$\bar{C}_D = \frac{\text{Drag}}{\frac{1}{2}\rho_\infty {u_\infty}^2 t}$$

Note: Symbols such as u, ρ, M, T refer to quantities measured at the edge of the viscous layer (boundary layer on wake). Ratios of velocity and density in the viscous layer to values at the edge of the layer are denoted by u^*, ρ^*.

The definitions of some of the symbols are illustrated in Fig. 1.

Subscripts

∞ Conditions in free stream

0 Conditions at separation

b Conditions on base

l Conditions at $x = l$

i Conditions reduced to incompressible flow

D Conditions on dividing streamline (except C_D, which see)

M Conditions on median streamline

B Conditions relevant to basic sharp-trailing-edge section

δ, a, w Subscripts to source distributions, *see* Section 4

REFERENCES

No.	*Author(s)*	*Title, etc.*
1	B. Thwaites (Ed.)	*Incompressible aerodynamics* (Fluid Motion Memoirs). Clarenden Press, 1960.
2	L. C. Woods	*The Theory of subsonic plane flow.* Cambridge University Press, 1961.
3	T. Yao-Tsu Wu	A wake model for free streamline flow theory. *J. Fluid Mech.*, Vol. 13, Part 2, p. 161. June, 1962.
4	A. N. Ivanov	Cavitation flow past airfoils. Isvestiia Akademii Nauk SSSR, Otdel. Tekh, Nauk, Mekhanika i Mashinostroenie, No. 6, p. 117, 1960. (Translation in *A.I.A.A. Journal*, Vol. 1, No. 1, p. 278. January, 1963.)
5	L. F. Crabtree	The formation of regions of separated flow on wing surfaces. Part 1, November, 1954. Part 2, July, 1957. A.R.C. R. & M. 3122.
6	J. F. Nash, V. G. Quincey and J. Callinan.	Experiments on two-dimensional base flow at subsonic and transonic speeds. A.R.C. R. & M. 3427. January, 1963.
7	D. R. Chapman	Reduction of profile drag at supersonic velocities by the use of airfoil sections having a blunt trailing edge. N.A.C.A. Tech. Note 3503. September, 1955.
8	H. H. Pearcey	Shock-induced separation and its prevention by design and boundary-layer control. (Part IV of *Boundary layer and flow control.* Editor, G. V. Lachmann.) Pergamon Press, 1961.
9	J. F. Nash	A review of research on two-dimensional base flow. A.R.C. R. & M. 3323. March, 1962.
10	A. Roshko	On the drag and shedding frequency of two-dimensional bluff bodies. N.A.C.A. Tech. Note 3169. July, 1954.
11	P. L. Poisson-Quinton and P. Jousserandot.	Influence du sufflage au voisinage du bord de fuite sur les caractéirstiques aerodynamiques d'une aile aux grandes vitesses. *La Recherche Aéronautique*, No. 56, p. 21. February, 1957.
12	A. M. O. Smith	Experimental investigation of the snow cornice or cusp effect for control of separation over blunt fairings. Douglas Aircraft Co. Inc., Engineering Department Rep. ES.26154. June, 1956.
13	M. Arie and H. Rouse ..	Experiments on two-dimensional flow over a normal wall. *J. Fluid Mech.*, Vol. 1, Part 2, p. 129. July, 1956.

REFERENCES—*continued*

No.	*Author(s)*	*Title, etc.*
14	C. J. Wood	Effect of base bleed on a periodic wake. *J.R.Ae.S.*, Vol. 68, p. 477. July, 1964.
15	T. H. Moulden	(Unpublished work.)
16	D. W. Holder	(Unpublished work.)
17	F. O. Ringleb	Separation control by trapped vortices. (Chapter in *Boundary layer and flow control.* Editor, G. V. Lachmann). Pergamon Press, 1961.
18	J. F. Nash	An analysis of two-dimensional turbulent base flow, including the effect of the approaching boundary layer. A.R.C. R. & M. 3344. July, 1962.
19	H. McDonald	Turbulent shear layer reattachment with special emphasis on the base pressure problem. *Aero. Quart.*, Vol. 15, p. 247. August, 1964.
20	J. C. Cooke	Separated supersonic flow. R.A.E. Tech. Note Aero. 2879. A.R.C. 24 935. March, 1963.
21	D. R. Chapman, D. M. Kuehn and H. K. Larson.	Investigation of separated flows in supersonic and subsonic streams with emphasis on the effect of transition. N.A.C.A. Report 1356. 1958.
22	H. H. Korst	A theory for base pressures in transonic and supersonic flow. *J. App. Mech.*, Vol. 23, No. 4, p. 593. December, 1956.
23	F. N. Kirk	An approximate theory of base pressure in two-dimensional flow at supersonic speeds. R.A.E. Tech. Note Aero. 2377. December, 1959.
24	J. C. Cooke	The boundary layer drag of slender wings and bodies in supersonic flow. R.A.E. Report Aero. 2661. A.R.C. 23 481. January, 1962.
25	J. Weber..	The calculation of the pressure distribution over the surface of two-dimensional and swept wings with symmetrical aerofoil sections. A.R.C. R. & M. 2918. July, 1953.
26	L. C. Woods	The application of the polygon method to the calculation of the compressible subsonic flow round two-dimensional profiles. A.R.C. C.P. 115. June, 1952.
27	H. Söhngen	Die Lösungen der Integralgleichung $$g(x) = \frac{1}{2\pi} \oint_{-a}^{a} \frac{f(\xi)d\xi}{x-\xi}$$ und deren Anwendung in der Tragflügeltheorie. *Mathematische Zeitschrift*, Heft 45, S.245. 1939.

REFERENCES—*continued*

No.	*Author(s)*	*Title, etc.*
28	N. I. Muskhelishvili	*Singular integral equations.* Publ. P. Noordhoff N. V.—Groningen—Holland. 1953.
29	J. F. Nash and V. G. Quincey ..	(Unpublished work.)
30	H. B. Squire and A. D. Young	The calculation of the profile drag of aerofoils. A.R.C. R. & M. 1838. November, 1937.
31	D. A. Spence	The growth of compressible turbulent boundary layers on isothermal and adiabatic walls. A.R.C. R. & M. 3191. June, 1959.
32	J. F. Nash	The effect of an initial boundary layer on the development of a turbulent free shear layer. A.R.C. C.P. 682. June, 1962.
33	H. W. Liepmann and J. Laufer	Investigation of free turbulent mixing. N.A.C.A. Tech. Note 1257. August, 1947.
34	R. C. Pankhurst and H. B. Squire.	Calculated pressure distributions for the R.A.E. 100–104 aerofoil sections. A.R.C. C.P. 80. March, 1950.
35	Edna M. Love and J. Williams	Additional data on surface slopes of the R.A.E. 100–104 aerofoil sections. A.R.C. C.P. 252. November, 1955.
36	K. Wieghardt	Erhöhung des turbulenten Reibungswiderstandes durch Oberflächenstörungen. *Forschungshefter für Schiffstechnik*, Heft 2, S.65. April, 1953.
37	J. F. Nash, T. H. Moulden and J. Osborne.	On the variation of profile drag coefficient below the critical Mach number. A.R.C. C.P. 758. November, 1963.
38	R. C. Lock	(Private communication.)
39	R. C. Maydew and J. F. Reed ..	Turbulent mixing of compressible free jets. *A.I.A.A. Journal*, Vol. 1, No. 6, p. 1443. June, 1963.
40	P. Bradshaw	The effect of initial conditions on the development of free shear layer. N.P.L. Aero Report 1117. September, 1964.
41	H. McDonald and I. A. Acklam	Some numerical results of the turbulent free shear layer with a finite initial boundary layer. British Aircraft Corporation (Warton) Report No. Ae. 212. June, 1964.
42	A. D. Young	The calculation of the profile drag of aerofoils and bodies of revolution at supersonic speeds. A.R.C. 15 970. April, 1953.
43	L. Howarth (Editor)	*Modern developments in fluid dynamics.* High speed flow. Clarendon Press. 1956.

APPENDIX

Derivation of Expression for C_D

Consider the flow in the upper half plane (Fig. A1), downstream of the trailing edge. Let Δ^* be the displacement thickness of the wake, defined by

$$\Delta^* = \int_0^\infty (1-\rho^* u^*) dy, \tag{A.1}$$

and Θ the momentum thickness, defined by

$$\Theta = \int_0^\infty \rho^* u^* (1-u^*) dy. \tag{A.2}$$

At the trailing edge the values of Δ^* and Θ can be related directly to the displacement thickness, δ_0^*, and momentum thickness, θ_0, of the boundary layer at separation:

$$\left.\begin{aligned} \Delta_0^* &= \delta_0^* + \tfrac{1}{2}h, \\ \text{and} \qquad \Theta_0 &= \theta_0. \end{aligned}\right\} \tag{A.3}$$

Far downstream of the section Δ^* and Θ tend to constant values, Δ_∞^* and Θ_∞, say, and it may be verified that their ratio tends to a value

$$\frac{\Delta_\infty^*}{\Theta_\infty} = 1 + (\gamma-1) M_\infty^2, \tag{A.4}$$

for a Prandtl number of unity. The asymptotic momentum thickness is a direct measure of the drag of the section (*see*, e.g. Woods[2]):

$$\Theta_\infty = \frac{c}{4} C_D. \tag{A.5}$$

The momentum-integral equation for the flow in the wake can be written

$$\frac{d}{dx}(\rho u^2 \Theta) = \Delta^* \frac{dp}{dx}, \tag{A.6}$$

since the shear stress vanishes along the streamline forming the centre line of the wake. This equation may be integrated from the trailing edge to infinity downstream to give

$$\Theta_\infty = \frac{\rho_0 u_0^2}{\rho_\infty u_\infty^2} \Theta_0 - \frac{C_{pb}}{2} \Delta_0^* - \frac{1}{2} \int_0^\infty C_p \frac{d\Delta^*}{dx} dx, \tag{A.7}$$

where the subscript $_0$ denotes conditions in the external stream at the separation point, and C_{pb} is the base-pressure coefficient. The external flow is equivalent to an inviscid flow past the displacement surface, and it is clear that the integral of the pressures, resolved in the stream direction, over the complete displacement surface must vanish[2]. Thus

$$\int_{-c}^\infty C_p \frac{d\Delta^*}{dx} dx = 0, \tag{A.8}$$

and therefore

$$\int_{-c}^0 C_p \frac{d\Delta^*}{dx} dx = -\int_0^\infty C_p \frac{d\Delta^*}{dx} dx. \tag{A.9}$$

Hence from equations (A.3), (A.7) and (A.9)

$$\Theta_\infty = \frac{\rho_0 u_0^2}{\rho_\infty u_\infty^2}\,\theta_0 - \frac{h + 2\delta_0^*}{4}\,C_{pb} + \frac{1}{2}\int_{-c}^{0} C_p \frac{d\Delta^*}{dx}\,dx. \tag{A.10}$$

The last two terms can be replaced by an integral taken round a circuit C comprising the part of the displacement surface upstream of the trailing edge and a line through the trailing edge normal to the chordline (Fig. A1):

$$\Theta_\infty = \frac{\rho_0 u_0^2}{\rho_\infty u_\infty^2}\,\theta_0 - \frac{h}{4}\oint C_p d\left(\frac{\Delta^*}{h}\right). \tag{A.11}$$

Equation (A.11) expresses, in effect, the total drag of the section as the sum of two terms, one a 'form drag' and the other the momentum deficit in the boundary layer. It is, in many respects, similar to the result derived by Cooke[24]. The result expressed in equation (A.11) is not, of course, restricted to aerofoils with thick trailing edges nor to symmetrical sections at zero incidence.

TABLE 1

I—Functions

x/l	$I_0(x/l)$	$I_1(x/l)$	$I_2(x/l)$
−5·0	−0·0597	−0·0348	−0·0249
−4·9	−0·0608	−0·0354	−0·0253
−4·8	−0·0619	−0·0362	−0·0258
−4·7	−0·0630	−0·0372	−0·0262
−4·6	−0·0642	−0·0380	−0·0267
−4·5	−0·0654	−0·0390	−0·0272
−4·4	−0·0668	−0·0394	−0·0278
−4·3	−0·0681	−0·0405	−0·0284
−4·2	−0·0696	−0·0410	−0·0289
−4·1	−0·0712	−0·0414	−0·0296
−4·0	−0·0728	−0·0421	−0·0302
−3·9	−0·0744	−0·0432	−0·0309
−3·8	−0·0760	−0·0445	−0·0316
−3·7	−0·0779	−0·0451	−0·0323
−3·6	−0·0798	−0·0461	−0·0331
−3·5	−0·0816	−0·0477	−0·0341
−3·4	−0·0838	−0·0484	−0·0347
−3·3	−0·0859	−0·0499	−0·0353
−3·2	−0·0882	−0·0511	−0·0365
−3·1	−0·0906	−0·0525	−0·0373
−3·0	−0·0931	−0·0540	−0·0380
−2·9	−0·0957	−0·0558	−0·0382
−2·8	−0·0986	−0·0573	−0·0396
−2·7	−0·1017	−0·0587	−0·0415
−2·6	−0·1049	−0·0606	−0·0424
−2·5	−0·1084	−0·0623	−0·0443
−2·4	−0·1120	−0·0645	−0·0452
−2·3	−0·1159	−0·0668	−0·0464
−2·2	−0·1201	−0·0691	−0·0480
−2·1	−0·1247	−0·0715	−0·0499
−2·0	−0·1296	−0·0741	−0·0518
−1·9	−0·1349	−0·0770	−0·0537
−1·8	−0·1407	−0·0801	−0·0558
−1·7	−0·1469	−0·0836	−0·0579
−1·6	−0·1538	−0·0873	−0·0603
−1·5	−0·1614	−0·0912	−0·0632
−1·4	−0·1697	−0·0958	−0·0659
−1·3	−0·1791	−0·1005	−0·0694
−1·2	−0·1894	−0·1061	−0·0727
−1·1	−0·2012	−0·1120	−0·0768
−1·0	−0·2146	−0·1187	−0·0813
−0·9	−0·2299	−0·1264	−0·0862
−0·8	−0·2477	−0·1352	−0·0918
−0·7	−0·2687	−0·1452	−0·0984
−0·6	−0·2936	−0·1572	−0·1057
−0·5	−0·3245	−0·1711	−0·1145
−0·4	−0·3632	−0·1881	−0·1248

TABLE 1—*continued*

x/l	$I_0(x/l)$	$I_1(x/l)$	$I_2(x/l)$
−0·3	−0·4142	−0·2091	−0·1373
−0·2	−0·4856	−0·2362	−0·1528
−0·1	−0·6002	−0·2733	−0·1727
0	−1·0000	−0·3333	−0·2000
0·1	−0·8965	−0·4230	−0·2423
0·2	−0·7848	−0·4903	−0·2981
0·3	−0·6631	−0·5323	−0·3597
0·4	−0·5284	−0·5447	−0·4179
0·5	−0·3768	−0·5217	−0·4609
0·6	−0·2008	−0·4538	−0·4723
0·7	0·0124	−0·3247	−0·4273
0·8	0·2911	−0·1005	−0·2804
0·9	0·7253	0·3194	0·0875
1·0	∞	∞	∞

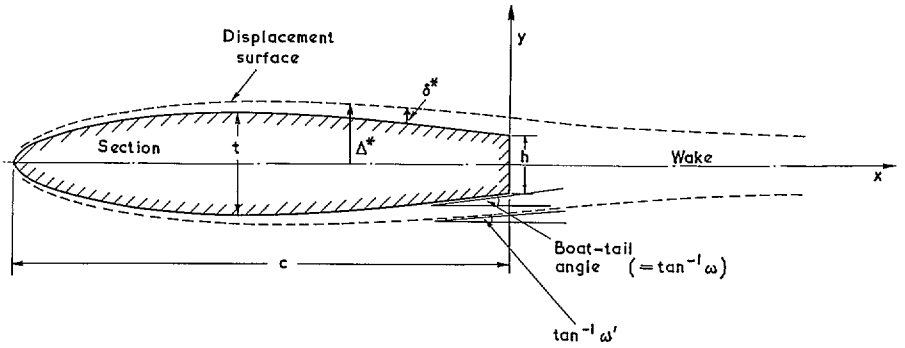

FIG. 1. Definitions of certain symbols.

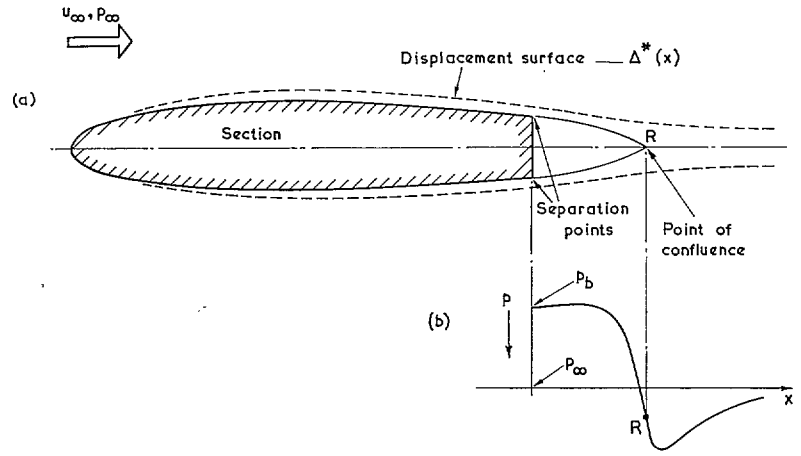

FIG. 2. The flow field and the pressure distribution in the wake (schematic).

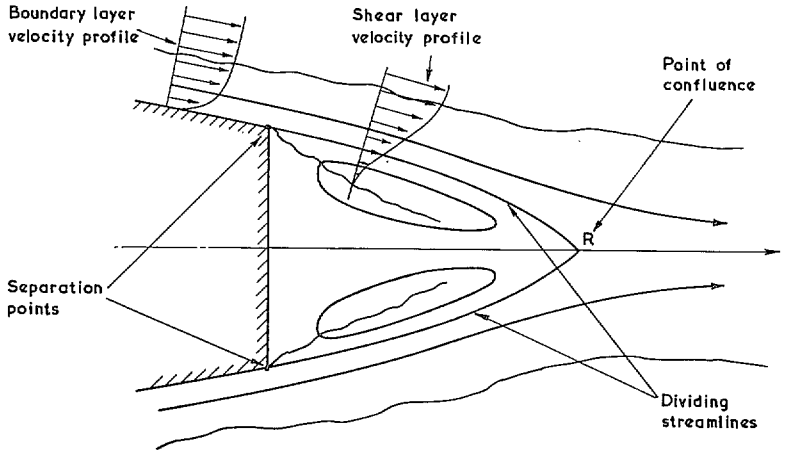

FIG. 3. Streamline pattern downstream of trailing edge (Schematic).

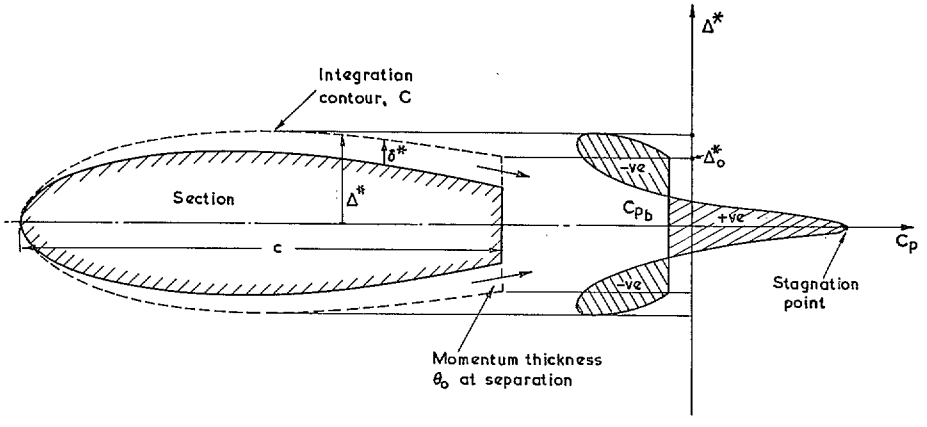

$$C_D = 4\,\frac{\rho_o}{\rho_\infty}\frac{u_o^2}{u_\infty^2}\,\frac{\theta_o}{c} - \frac{1}{c}\int C_p\, d\,\Delta^*$$

FIG. 4. Method of determining C_D from pressure distribution.

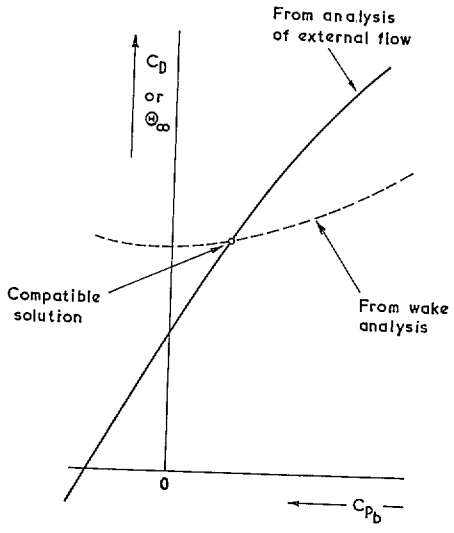

FIG. 5. Solution for C_D and C_{pb} to satisfy external flow and wake development (schematic).

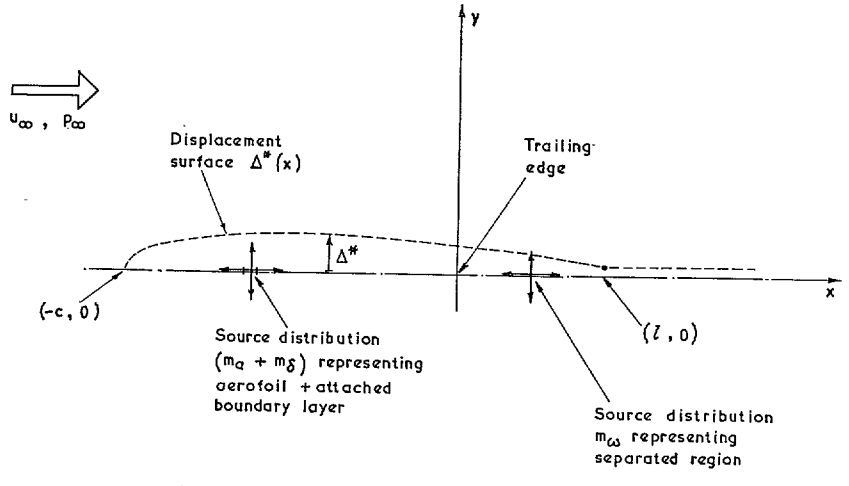

FIG. 6. Model for analysis of external flow.

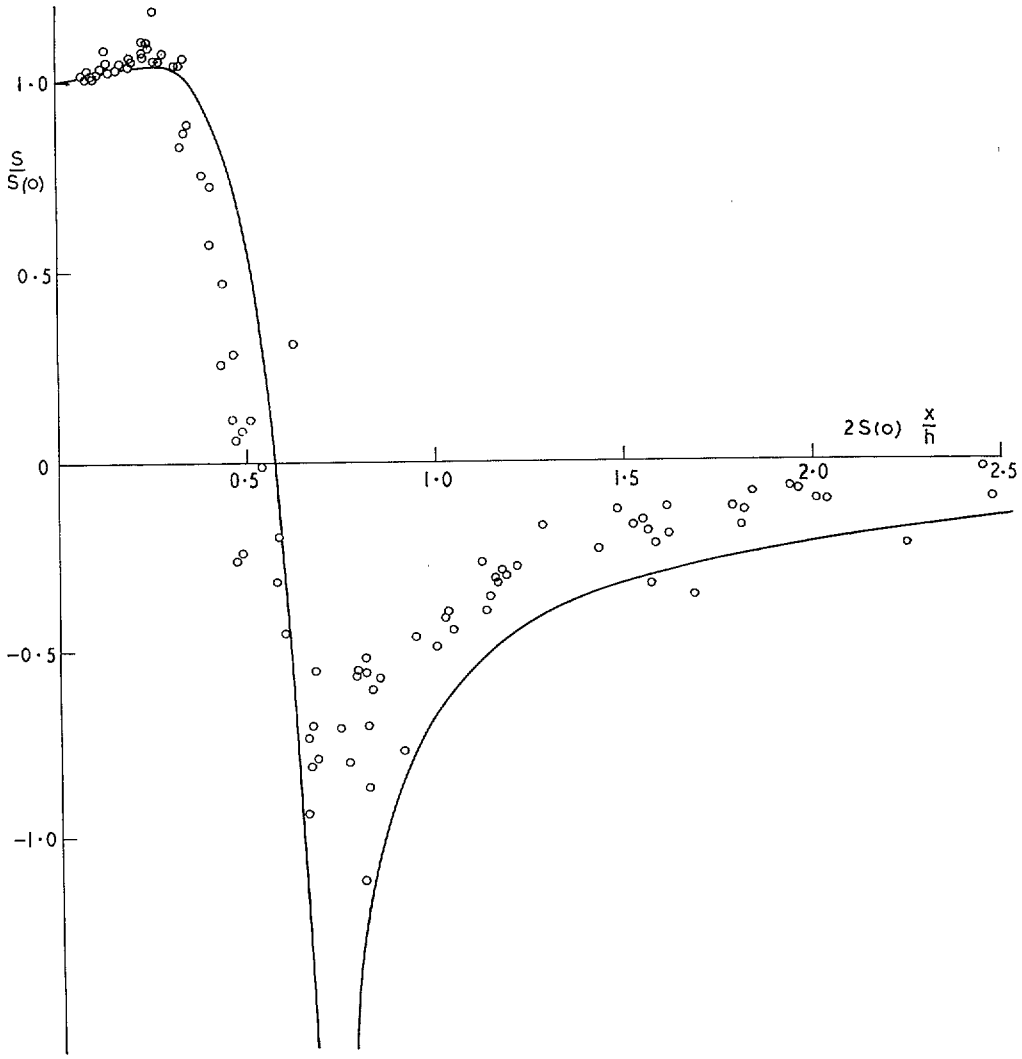

FIG. 7. The pressure distribution downstream of a step—correlation of experimental data.

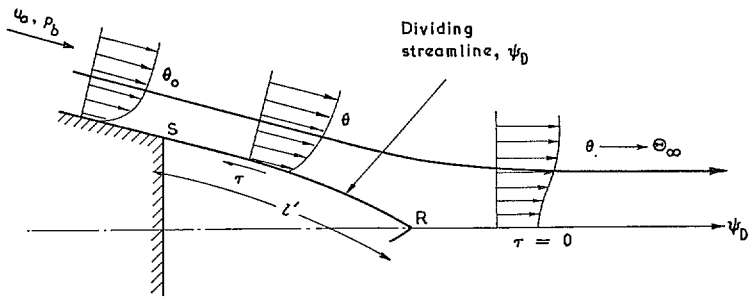

FIG. 8. Model for analysis of wake.

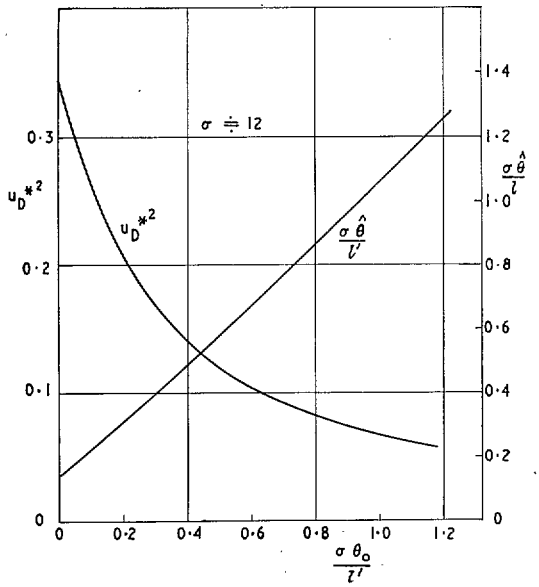

FIG. 9. Computed results for the pre-asymptotic turbulent free-shear layer.

($u_D{}^*$ = velocity on dividing streamline

θ_0 = momentum thickness at separation ($x = 0$)

$\hat{\theta}$ = momentum thickness of shear layer outboard of dividing streamline at $x = l'$).

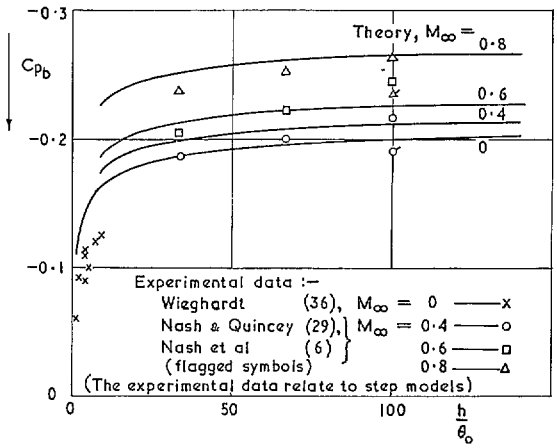

FIG. 10. Variation of base pressure with ratio of base height to boundary-layer momentum thickness—semi-infinite, parallel-sided section.

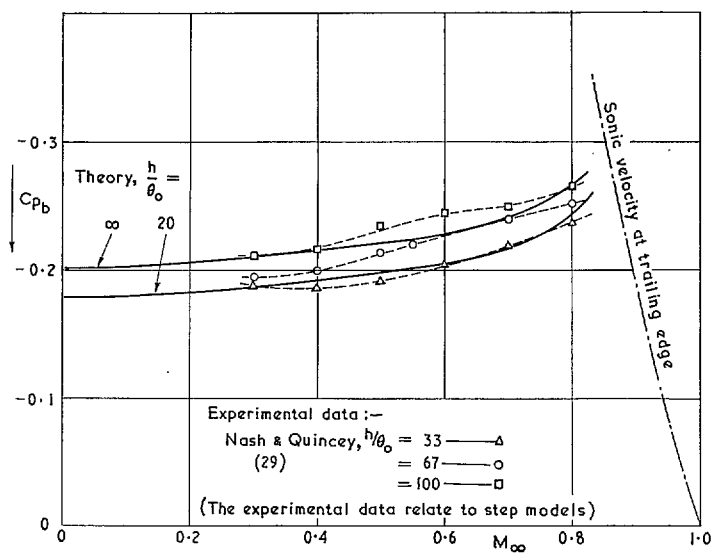

FIG. 11. Variation of base pressure with Mach number—semi-infinite, parallel-sided section.

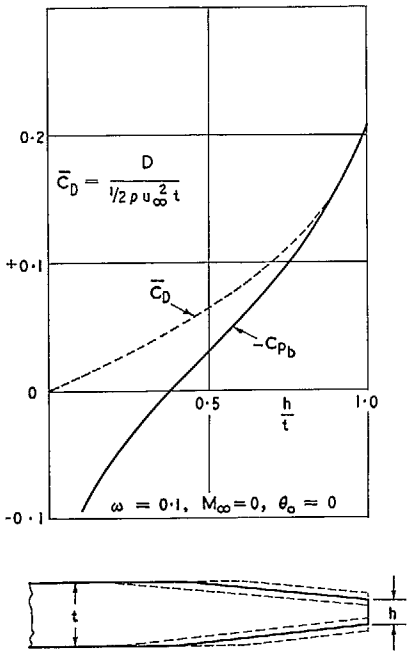

FIG. 12. Effect of boat-tailing on base pressure—constant boat-tail angle (= 5·71°).

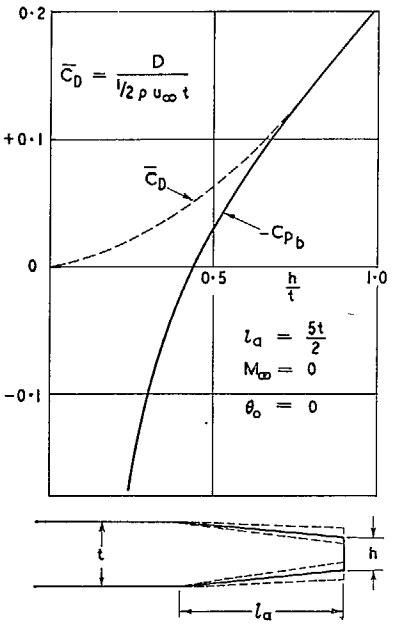

FIG. 13. Effect of boat-tailing on base pressure—constant-length afterbody (= $2\frac{1}{2}$ × max. thickness).

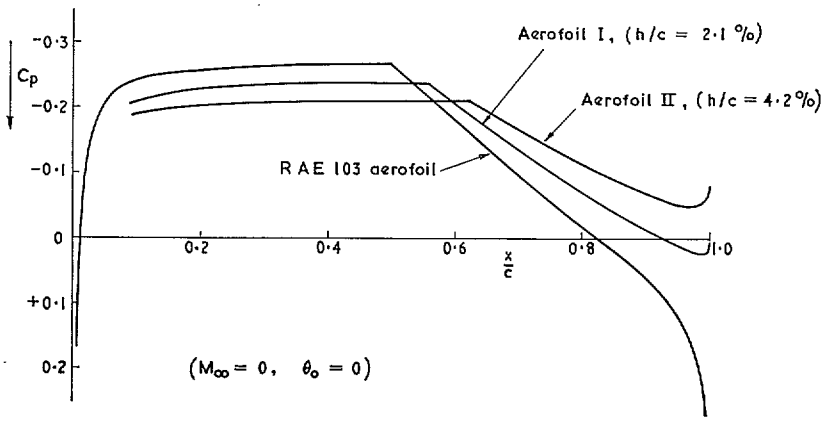

FIG. 14. Predicted pressure distributions round three 10 per cent thick aerofoil sections.

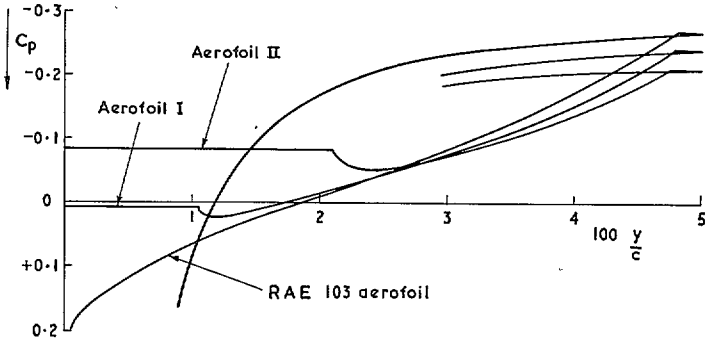

FIG. 15. Predicted pressure distributions in terms of ordinate normal to chordline.

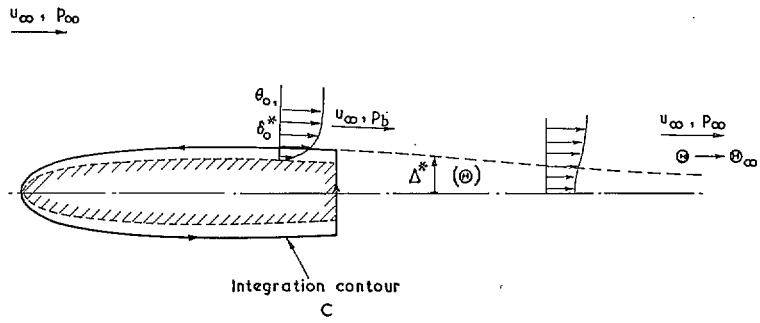

FIG. A1. Model for derivation of expression for C_D.

(92793) Wt. 67/7689 K5 9/66 Hw.

Publications of the Aeronautical Research Council

ANNUAL TECHNICAL REPORTS OF THE AERONAUTICAL RESEARCH COUNCIL (BOUND VOLUMES)

1945 Vol. I. Aero and Hydrodynamics, Aerofoils. £6 10*s*. (£6 14*s*.)
Vol. II. Aircraft, Airscrews, Controls. £6 10*s*. (£6 14*s*.)
Vol. III. Flutter and Vibration, Instruments, Miscellaneous, Parachutes, Plates and Panels, Propulsion. £6 10*s*. (£6 14*s*.)
Vol. IV. Stability, Structures, Wind Tunnels, Wind Tunnel Technique. £6 10*s*. (£6 14*s*.)

1946 Vol. I. Accidents, Aerodynamics, Aerofoils and Hydrofoils. £8 8*s*. (£8 12*s*. 6*d*.)
Vol. II. Airscrews, Cabin Cooling, Chemical Hazards, Controls, Flames, Flutter, Helicopters, Instruments and Instrumentation, Interference, Jets, Miscellaneous, Parachutes. £8 8*s*. (£8 12*s*.)
Vol. III. Performance, Propulsion, Seaplanes, Stability, Structures, Wind Tunnels. £8 8*s*. (£8 12*s*.)

1947 Vol. I. Aerodynamics, Aerofoils, Aircraft. £8 8*s*. (£8 12*s*. 6*d*.)
Vol. II. Airscrews and Rotors, Controls, Flutter, Materials, Miscellaneous, Parachutes, Propulsion, Seaplanes, Stability, Structures, Take-off and Landing. £8 8*s*. (£8 12*s*. 6*d*.)

1948 Vol. I. Aerodynamics, Aerofoils, Aircraft, Airscrews, Controls, Flutter and Vibration, Helicopters, Instruments, Propulsion, Seaplane, Stability, Structures, Wind Tunnels. £6 10*s*. (£6 14*s*.)
Vol. II. Aerodynamics, Aerofoils, Aircraft, Airscrews, Controls, Flutter and Vibration, Helicopters, Instruments, Propulsion, Seaplane, Stability, Structures, Wind Tunnels. £5 10*s*. (£5 14*s*.)

1949 Vol. I. Aerodynamics, Aerofoils. £5 10*s*. (£5 14*s*.)
Vol. II. Aircraft, Controls, Flutter and Vibration, Helicopters, Instruments, Materials, Seaplanes, Structures, Wind Tunnels. £5 10*s*. (£5 13*s*. 6*d*.)

1950 Vol. I. Aerodynamics, Aerofoils, Aircraft. £5 12*s*. 6*d*. (£5 16*s*. 6*d*.)
Vol. II. Apparatus, Flutter and Vibration, Meteorology, Panels, Performance, Rotorcraft, Seaplanes. £4 (£4 3*s*. 6*d*.)
Vol. III. Stability and Control, Structures, Thermodynamics, Visual Aids, Wind Tunnels. £4 (£4 3*s*. 6*d*.)

1951 Vol. I. Aerodynamics, Aerofoils. £6 10*s*. (£6 14*s*.)
Vol. II. Compressors and Turbines, Flutter, Instruments, Mathematics, Ropes, Rotorcraft, Stability and Control, Structures, Wind Tunnels. £5 10*s*. (£5 14*s*.)

1952 Vol. I. Aerodynamics, Aerofoils. £8 8*s*. (£8 12*s*.)
Vol. II. Aircraft, Bodies, Compressors, Controls, Equipment, Flutter and Oscillation, Rotorcraft, Seaplanes, Structures. £5 10*s*. (£5 13*s*. 6*d*.)

1953 Vol. I. Aerodynamics, Aerofoils and Wings, Aircraft, Compressors and Turbines, Controls. £6 (£6 4*s*.)
Vol. II. Flutter and Oscillation, Gusts, Helicopters, Performance, Seaplanes, Stability, Structures, Thermodynamics, Turbulence. £5 5*s*. (£5 9*s*.)

1954 Aero and Hydrodynamics, Aerofoils, Arrester gear, Compressors and Turbines, Flutter, Materials, Performance, Rotorcraft, Stability and Control, Structures. £7 7*s*. (£7 11*s*.)

Special Volumes

Vol. I. Aero and Hydrodynamics, Aerofoils, Controls, Flutter, Kites, Parachutes, Performance, Propulsion, Stability. £6 6*s*. (£6 9*s*. 6*d*.)
Vol. II. Aero and Hydrodynamics, Aerofoils, Airscrews, Controls, Flutter, Materials, Miscellaneous, Parachutes, Propulsion, Stability, Structures. £7 7*s*. (£7 10*s*. 6*d*.)
Vol. III. Aero and Hydrodynamics, Aerofoils, Airscrews, Controls, Flutter, Kites, Miscellaneous, Parachutes, Propulsion, Seaplanes, Stability, Structures, Test Equipment. £9 9*s*. (£9 13*s*. 6*d*.)

Reviews of the Aeronautical Research Council

1949–54 5*s*. (5*s*. 6*d*.)

Index to all Reports and Memoranda published in the Annual Technical Reports

1909–1947 R. & M. 2600 (out of print)

Indexes to the Reports and Memoranda of the Aeronautical Research Council

Between Nos. 2451–2549: R. & M. No. 2550 2*s*. 6*d*. (2*s*. 9*d*.); Between Nos. 2651–2749: R. & M. No. 2750 2*s*. 6*d*. (2*s*. 9*d*.); Between Nos. 2751–2849: R. & M. No. 2850 2*s*. 6*d*. (2*s*. 9*d*.); Between Nos. 2851–2949: R. & M. No. 2950 3*s*. (3*s*. 3*d*.); Between Nos. 2951–3049: R. & M. No. 3050 3*s*. 6*d*. (3*s*. 9*d*.); Between Nos. 3051–3149: R. & M. No. 3150 3*s*. 6*d*. (3*s*. 9*d*.); Between Nos. 3151–3249: R. & M. No. 3250 3*s*. 6*d*. (3*s*. 9*d*.); Between Nos. 3251–3349: R. & M. No. 3350 3*s*. 6*d*. (3*s*. 11*d*.)

Prices in brackets include postage

Government publications can be purchased over the counter or by post from the Government Bookshops in London, Edinburgh, Cardiff, Belfast, Manchester, Birmingham and Bristol, or through any bookseller

Printed and published by
HER MAJESTY'S STATIONERY OFFICE

To be purchased from
49 High Holborn, London WC1
423 Oxford Street, London W1
13A Castle Street, Edinburgh 2
109 St. Mary Street, Cardiff
Brazennose Street, Manchester 2
50 Fairfax Street, Bristol 1
35 Smallbrook, Ringway, Birmingham 5
80 Chichester Street, Belfast 1
or through any bookseller

Printed in England

S.O. Code No. 23-3436